# TAILORING OF GROWTH FACTOR RELEASE FROM ELECTROSPUN HYDROGEL MICROFIBERS FOR APPLICATIONS IN REGENERATIVE MEDICINE

by
Brook Jeang

A thesis submitted to Johns Hopkins University in conformity with the requirements for the degree of Master of Science in Engineering

Baltimore, Maryland
August, 2015

## Abstract

Tissue engineering, the primary therapeutic approach to achieving regeneration following traumatic injury or disease, is a complex undertaking. As the therapeutic window of most neurotrophic factors remains largely unknown, a simple, flexible platform is necessary in order to bioassay neurotrophic factors and determine how their complex interplay influences cellular response and regenerative processes. Factors such as scaffold material, topographic cues, incorporation of cells, and delivery of biochemical signals must all be considered in order to design a successful engineered graft that allows for these aspects to be studied in a single, inclusive system. Thus, we have developed an easily scalable method of surface modifying electrospun hydrogel microfibers to further enhance the utility of aligned hydrogels used in tissue regeneration. Using EDC/NHS coupling, we are able to conjugate heparin to the surface of any biopolymer hydrogel that contains primary amines in order to achieve sustained release of biochemical cues at the target site. Topographic cues are presented via the scaffold itself; the hydrogel environment mimics the native extracellular matrix and provides a 3D culture environment for cells. Additionally, electrospinning induces alignment of fibers, which increases the strength of our scaffolds while directing cell growth in the orientation of the fibers. Finally, surface modification of electrospun fibers with heparin allows for the capture and controlled delivery of growth factors without affecting the properties of the biopolymer and, by consequence, altering hydrogel formation. Neural stem cells seeded as spheroids onto unmodified electrospun fibrin hydrogel scaffolds were observed migrating out and spreading in the direction of fibers. We found that heparin itself inhibited cell outgrowth and spreading, but capture of glial-derived neurotrophic factor by heparin when GDNF was presented in concentrations as low as 2 ng/ml appeared to counteract inhibition by heparin alone and promote cell spreading. Astrocytes and neurons were both detected at D21 on heparinized fibers, regardless of extent of spreading on fibers, whereas by D21, nonheparinized fibers stained positive almost exclusively for neurons. As astrocytes have the ability to enhance neuronal survival and regeneration, the presence of both neurons and astrocytes in culture can be potentially useful in developing therapies for neurodegenerative diseases.

## Acknowledgements

I would first and foremost like to thank the Department of Materials Science and Engineering for allowing me to continue my studies and pursue my Master's. I must thank Jeanine Majewski for her patience and assistance throughout all of my time at Hopkins. On behalf of all of the students who pass through the department, thank you for your dedication to helping make our department run as smoothly as possible. I would also like to thank Dr. Orla Wilson and Dr. John Baty. Your lectures time and time again revived my interest in the field, but more significantly, your warmth and guidance have brightened my Hopkins experience immeasurably.

I cannot begin to express how grateful I am to my PI, Dr. Hai-Quan Mao, without whom this thesis would not have been possible. Despite every experiment that didn't go as planned and all of the unanswered questions following each of my lab presentations, your support never wavered. Thank you for providing me with the opportunity to learn and grow throughout these last three years – it has been such an incredible honor and blessing to work in the lab of a professor who is so compassionate and involved. I will carry the lessons and skills I have amassed over the course of my time in the Mao lab with me through all my future endeavors.

Thank you to the Mao lab for welcoming me and fostering an environment so conducive to collaboration and learning. I must thank the many post-docs in our lab who I have consulted on innumerous occasions. Thank you to Drs. Jisuk Choi, Xuesong Jiang, and Xiaowei Li for patiently answering all of my questions and providing invaluable feedback; I have learned so very much from each of you.

My experience in the Mao lab began with a meeting with Brian Ginn, and thus I find it fitting that I round off my thank yous to members of the lab by expressing my deepest gratitude to him. I am so blessed to have had such a hands-on mentor who dedicated so much time and energy to guide me through every aspect of my research, via countless email correspondences, the never-ending supply of questions I always seem to have, innumerable modifications of experiments, and everything in between. Your hard work and dedication are admirable and unparalleled; I hope to be even a fraction as industrious as you are in all that I take on.

I must also thank my former teachers and life mentors who have all played indispensable roles in guiding me along this journey. A million thank yous for the lessons you've imparted that have led me to

this point. I don't know where I would be without my incredible friends. To quote A.A. Milne, "I knew when I met you an adventure was going to happen." Thank you for giving me the strength to carry on through the roughest of times, celebrating every little success with me, and growing with me as we travel along this road.

Finally, I would but utterly lost without my ineffably wonderful and supportive family. Thank you to my grandparents for your unconditional love and support. You have always been a prime example for the lifestyle I strive to lead. Thank you, Aunt Ti, for sparking my interest in science and being my lifeline on the East Coast. You helped quell the most acute bouts of homesickness and made Maryland feel like home these past 5 years. None of this would have been remotely possible without my greatest role models and supporters: my parents, Dwan Lin and Fure-Lin Jeang. It has been difficult being so far from home for so long, but I know that each struggle I have encountered, you have felt ten-fold. You have sacrificed everything to provide me with a blessed life, equipped with all of the tools I need to succeed. There are no words that can fully capture how grateful and honored I am to be your daughter. I love you.

## Table of Contents

## List of Tables

## List of Figures

## 1. Introduction

Bioengineered grafts with properties that can be tuned to address specific, clinical needs have been widely studied and sought after as an alternative to autografts, the clinical gold standard in many tissue engineering applications such as cardiac, vascular, orthopedic, spinal cord, and musculoskeletal regeneration.[1] Autotransplantation involves the harvesting of bone or tissue from donor sites within the patient. While there is no risk of disease transfer or rejection of autografts, there are a multitude of challenges associated with transplantation of autografts, including the need for a secondary injury, donor site morbidity, limited availability of sufficiently sized autograft material for optimal repair, and variability of autograft efficiency.[2] In the context of nerve regeneration, nerve guidance conduits (NGCs) are the primary engineering solution to circumventing additional surgery and comorbidities, thus potentially matching or outperforming nerve autografts. NGCs guide axonal sprouting from the proximal to distal stump, prevent neuroma formation and excessive branching, and protect the injury site. Successful NGCs should be capable of concentrating neurotrophic factors, reducing cellular invasion and scarring of the nerve, and mimicking the native extracellular matrix (ECM), which consists of an intricate network of glycosaminoglycans, structural proteins, and matricellular proteins.[3] This network works together to carry out complex signaling events and provide structural support for many cellular processes. A myriad of factors must be considered in the design of NGCs in order to provide a favorable, ECM-like microenvironment to improve nerve regeneration. To facilitate the exchange of nutrients between the lumen and outer environment, engineered grafts must be semi-permeable. They must also be constructed of reabsorbable biomaterials for successful long-term recovery. Materials selection becomes a critical factor when tailoring degradation rates of NGCs for specific applications, as it is assumed that the release of a protein or drug from NGCs follows polymer degradation kinetics.[4] NGC materials are generally categorized as nonresorbable or resorbable, the latter being of greater interest in creating the ideal nerve conduit. Biodegradable materials commonly used in NGCs include collagen, gelatin, fibrin, alginate, polyglycolic acid, and chitosan.[5] Another design aspect to consider is incorporation of cells and growth factors into artificial nerve grafts. Cells secrete their own neurotrophic factors and express cell-adhesion molecules to enhance regeneration by promoting neurite outgrowth and neuronal survival. Neurotrophic factors such as brain-derived neurotrophic factor (BDNF) and nerve growth factor (NGF) increase dendritic

and axonal branching as well as the number and localization of synaptic vesicles at the site of neurotransmitter release. Meanwhile, cell adhesion molecules influence synapse formation by inducing synapse specification, adhesion, and signaling. They also induce pre-synaptic and post-synaptic differentiation.[6] These endogenous biomolecules can be further supplemented by the exogenous growth factors delivered to the target site.[2] Since the effects of growth factors are dose-dependent, their therapeutic windows and labyrinthine biological effects must be studied carefully to select the most suitable factors in appropriate quantities to optimize regeneration.

To match or surpass the performance of autografts, scaffolding in tissue engineering must mimic the structure and functions of the native ECM. In native tissue, ECM provides structural support for cells, supplies growth factors and potentiates their activity, provides bioactive cues to cells to respond to their microenvironment, and imparts mechanical strength to tissues.[7] The vast variety of scaffold choices for tissue engineering is best narrowed down by considering the desired application for the scaffold. Hydrogels, for instance, are a principal scaffold material used for constructing artificial nerve grafts. These swollen networks are lightly cross-linked polymer chains that can be reversibly dehydrated and reswollen depending on environmental conditions, thereby enabling drug uptake and release.[5] Hydrogel scaffolds must provide specific structural, mechanical, and biochemical cues to cells in a controlled manner in order to guide cells spatially and temporally towards tissue formation and nerve regeneration.[5] Mechanical and physical features that influence the efficacy of a hydrogel for tissue regeneration include the overall architecture, physical dimensions, strength, stiffness, mesh size, and porosity of the gel as well as the biomaterials used in constructing the gel. Biocompatibility with tissues and release of therapeutic agents also play critical roles in hydrogel performance. These features must all be carefully evaluated when designing and constructing ECM-like hydrogel scaffolds that provide mechanical support for dendritic growth as well as biological signals to direct axonal growth towards the distal stump in nerve regeneration.[5]

Due to its relative simplicity and versatility, electrospinning is a popular technique used to generate random or aligned nanofibers for tissue engineering applications. Fiber diameter influences cell proliferation and migration; migration is limited essentially to the surface of scaffolds for fiber diameters below 0.25 $\mu$m, while optimal depth migration and proliferation is believed to occur on fibers with

diameters above 2 $\mu$m.[8] Using electrospinning, we are able to easily tune fiber diameter as well as reproducibly create fibers with diameters on the micron scale. High biocompatibility, biodegradability, reproducibility, scalability, and cost effectiveness are additional factors that are considered in designing electrospun fibrous scaffolds that not only bear strong morphological resemblance to the native ECM but also function as delivery systems. Fibers can be made from a wide range of starting natural materials, including fibrin, alginate, gelatin, and hyaluronic acid, which are selected to match the properties and projected time of regeneration of the injured tissue or nerve.[9, 10] The elastic modulus of central nervous system tissue is typically reported in the range of 3-300 kPa for spinal cord tissue and approximately 500 Pa for brain tissue, making highly swollen yet easy to handle electrospun hydrogels an ideal choice for scaffolding material.[11] The loose bonding between electrospun fibers is also believed to stimulate tissue growth and cell migration, while encapsulation of growth factors within electrospun scaffolds can potentially further improve regeneration.[4] The basis of electrospinning entails applying a high voltage to a polymer solution that is extruded at a fixed rate. As the droplet at the needle tip becomes highly electrified, the applied electric field overcomes the solution viscosity and tends to form a Taylor cone. When the electric field threshold is surpassed, a finely charged polymer jet emerges from the tip of the Taylor cone and sprays as a continuous fiber onto a grounded collector.[12]

We utilize a variation of the classic electrospinning technique to generate hydrogel microfibers (**Appendix 1**).[10] Aqueous polymer solutions are extruded into a rotating collection bath where they are rapidly cross-linked to form hydrogel microfibers. Spinning onto a wet cross-linking bath rather than a dry collecting sheet allows us to easily alter cross-linking density. Alignment of fibers is a combined result of electrical and mechanical stretching. The electric field applied to the polymer solution induces dipole alignment of polymer chains, while the rotation of the collection wheel mechanically stretches the polymer jet as it lands in the cross-linking solution. Fiber diameter can be manipulated by adjusting separation distance between polymer jet and collection wheel as well as weight percent of material spun. Additional factors that influence fiber diameter include rotation speed of the collection bath and solution extrusion rate, such that at lower rotation speeds and lower extrusion rates, microfibers rather than nanofibers are formed. Uniaxial alignment of hydrogel fibers synthesized using this method has previously been

confirmed using scanning electron microscopy and small angle X-ray scattering and shown to improve the mechanical properties of the hydrogel fibers.[10]

In this study, fibrin hydrogels were formed using this modified electrospinning method. Fibrinogen is a rod-shaped protein with molecular weight of 340 kDa and can be obtained autologously, thus significantly reducing potential risks of foreign body reaction and viral infection.[13] Thrombin-mediated cross-linking converts fibrinogen into stable fibrin networks. Fibrin and fibrinogen play prominent roles in pathological processes such as wound healing, inflammatory response, cellular and matrix interactions, blood clotting, fibrinolysis, and neoplasia. Fibrin scaffolds are most widely used in the form of hydrogels, microbeads, and glues (commercially sold as Tissucol/Tisseel®, Evicel®, and Crosseal™).[15] Furthermore, due to its great biocompatibility and biodegradability, fibrin has been used as a hemostatic agent in clinical cardiac, spleen, and liver surgeries.[12] Cells entrapped in fibrin gel have been shown to produce more collagen and elastin, which confer structural support.[13] The utility of fibrin scaffolds can be further improved by the incorporation of biologically active materials to facilitate cell adhesion. Despite the excellent versatility and biocompatibility of fibrin scaffolds, setbacks include loss of shape due to disintegration of gels before proper regeneration and low mechanical stiffness.[14] Using the altered electrospinning method described above, we were able to synthesize fibrin hydrogels of suitable mechanical strength, stiffness, and cross-linking density to combat these reported disadvantages without any loss of adaptability or compromised functionality.

We aimed to incorporate biochemical cues into our hydrogel scaffolds in order to augment their utility and functionality. Commonly used methods of loading biomolecules into electrospun fibers include submerging scaffolds in an aqueous phase of proteins, blend electrospinning, and coaxial electrospinning. Dipping scaffolds into soluble protein soak baths allows proteins to attach directly via physical absorption with little interference to the bioactivity of the loaded biomolecules. However, uncontrolled release profiles present risks such as toxicity, burst release of drugs, and low reproducibility. Blend, or emulsion, electrospinning involves mixing proteins directly with polymer solutions prior to electrospinning. While this is seen as a relatively facile approach, protein distribution on the fibers tends to be heterogeneous and a decrease in the bioactivity of the loaded protein is frequently observed. Neither method is suitable for the highly aqueous fibers we generate using our electrospinning setup, as any proteins spun with the polymeric

scaffolding material quickly diffuse out into the collection bath of much greater volume. Furthermore, the stability of the fibers themselves can be compromised by the addition of proteins to the precursor solution. Coaxially electrospun fibers are generated by simultaneously and coaxially electrospinning the polymer and protein solutions through different inlet channels into one nozzle to for a core-shell structure. The resultant fibers have a homogeneous protein distribution throughout the fibers.[4] Due to electric charges being located primarily at the outer fiber surface, inner protein solutions are shielded from degradation by this shell barrier. Release profiles from coaxial electrospun fibers indicate initial burst release followed by a stage of sustained release, likely due to the longer diffusion path through the core-shell structure. Despite this, the physical entrapment of proteins in the core of coaxial electrospun fibers still does not address the short biological half-life of proteins. Additionally, proteins that are charge sensitive may be difficult to incorporate into the actual electrospinning process or affect assembly and mechanical strength of fibers.[16] Thus, we sought a method of binding growth factors to the surfaces of our hydrogel fibers post-electrospinning in order to enhance capture and retention of soluble factors present in soak solution.

Covalent immobilization has been shown in the literature to retain growth factors for longer periods of time at the target site.[17] Free diffusion is hindered when growth factors are tethered to scaffolds, thereby offering control over the amount and distribution of biochemical cues in delivery systems. As immobilizing growth factors prolongs growth factor release, biological activity must be maintained for the duration of the projected regeneration time. Initial burst release can inhibit axonal sprouting by downregulating growth factor receptors and thus reducing affinity binding of these receptor sites to growth factors.[18] In order to develop efficient neurotrophic factor delivery systems, problems of protein instability, control over release kinetics, and unclear therapeutic windows must be elucidated. Loss of bioactivity may arise from blockage of specific functional groups on growth factors via chemical conjugation to scaffolds. Compromised biological activity not only detracts from the therapeutic potential of a delivery system but can also induce negative immunogenic effects. Furthermore, inadequate dosage and ill-defined release kinetics can lead to aberrant axonal growth. Finally, while it is widely accepted that neurotrophic factor effects are dose-dependent, the complicated interplay of neurotrophic factors present in regenerative processes remains largely unknown. Therefore, selecting a facile yet efficient conjugation reaction that can easily be scaled up

to broadly assay the effects of soluble, heparin-binding neurotrophic factors on cellular response in a host of tissue engineering applications is a critical factor in the development of delivery systems.

One class of affinity-based delivery system that is frequently employed exploits heparin as a carrier of biomolecules. With respect to fibrin scaffolds, heparin-immobilized neurotrophin-3 within fibrin gels has been shown to enhance neuronal outgrowth from chick dorsal root ganglia (DRGs) and increase neural fiber density in rat spinal cord lesions. Likewise, enhanced neurite extension from chick DRGs placed inside fibrin matrices containing $\beta$-NGF bound to heparin has been reported.[19-21] Heparin is a linear polysaccharide that is comprised of alternating hexuronic acid and glucosamine residues.[22] It has broad uses in biomedical applications, including drug delivery, cell differentiation, reducing material thrombogenicity, and promoting material self-assembly. Heparin is capable of interacting strongly with different proteins in very specific manners as a result of its unique structure and surface charge distribution. It has been shown to sequester endogenous growth factors secreted *in vitro* or in *vivo*, and protects proteins that contain heparin-binding sites from degradation by stabilizing and immobilizing them within biomaterial matrices. Growth factors bind electrostatically to the carboxylic acid and acidic sulfate moieties on heparin through their heparin-binding domains.[10] The binding of proteins to heparin-based delivery systems *in vitro* mimics the interactions between growth factors and delivery systems that occur naturally within native ECM proteoglycans. Controlled growth factor release in heparin-affinity systems is moderated by enzymatic degradation of scaffolds, underscoring the importance of fiber degradation as a scaffold design factor. Accordingly, heparin was selected as a drug carrier for our study due to the stability, flexibility, and scalability it affords. Additionally, many central nervous system growth factors contain heparin-binding domains, including glial cell-derived neurotrophic factor (GDNF), bFGF, BDNF, neuregulin (NRG), and vascular endothelial growth factor (VEGF).[23, 24] Surface modification of fibrin scaffolds was carried out using 1-ethyl-3-(3-dimethylaminopropyl)carbodiimide (EDC), which was used to activate the carboxyl groups in heparin. Activated heparin was then reacted with the primary amines on the surface of the fibrin fibers. This method of surface modification using heparin takes place after electrospinning; therefore, the stability of the hydrogel fibers remains unperturbed. Furthermore, this heparinization approach can be employed to functionalize any biopolymer hydrogel that contains either

primary amines or carboxylic acid groups when a diamine linker is used, making it a suitable choice for a variety of tissue engineering applications.

Neurotrophic factors (NTFs) are polypeptides that are known to regulate nerve cell survival and differentiation in both peripheral and central nervous system development. NTFs in circulation have inadequate release kinetics and short biological half-lives, typically on the order of minutes to a few hours at best depending on the particular growth factor. Drug delivery systems are thus designed to provide sustained release of sufficient concentrations of bioactive NTFs at target sites while protecting them from rapid degradation *in vivo*.[3] Biological processes are influenced by the concerted actions of many NTFs. Accordingly, in the delivery of multiple therapeutic agents, the different time courses of release required for each factor must be optimized. While it is known that NTFs generally influence cell behavior at very low concentrations in the range of $10^{-9}$ to $10^{-11}$ M, proper design must also consider that NTFs usually elicit biphasic responses. At low concentrations, NTF dosage is insufficient to activate cells. At high concentrations, the amount of NTF presented saturates receptors and can be toxic to cells.[13] It follows that the selection of optimal therapeutic agents in appropriate doses for specific applications is another key factor in improving the performance of delivery systems.

Extensive bioassays are required to understand the therapeutic windows and complex interactions among neurotrophic factors that remain largely unknown. Hence, choice of cell line and relevant neurotrophic factors are critical design factors. Neural stem cells are self-renewing, multipotent cells that can proliferate and generate the main cell lineages of the nervous system: neurons, astrocytes, and oligodendrocytes. They are considered the optimal cell type for cell mediated therapy of neural disorders, as they are derived from the same tissue as damaged cells and display strong responsiveness to local environmental cues. Evidence suggesting that human neural stem cells (hNSCs) secrete GDNF, BDNF, VEGF, and insulin-like growth factor 1 (IGF-1), provides hope that they may protect dysfunctional motor neurons and increase dopaminergic neuron survival in animal models of neurodegenerative disease.[25] Thus, great effort has been invested in developing neural stem cell based strategies of treatment for neurodegenerative diseases and stroke. Transplantation of neural stem cells has been explored for treatment of Parkinson's disease, Alzheimer's disease, spinal cord injury, Huntington's disease, and multiple sclerosis while the delivery of human neural stem cells at multiple sites along the spinal cord has been

investigated for treatment of amyotrophic lateral sclerosis. Neural stem cells have also been modified to produce necessary cytokines to treat brain tumors and cell replacement therapy using hNSCs has been studied for treating stroke patients.[25]

For our study, we first studied the effects of GDNF on NSC proliferation. GDNF is a key factor for motor axonal regeneration due to its ability to promote axonal elongation and survival.[3] GDNF was captured by fibrin scaffold surfaces modified with heparin in order to study differences in cellular response when growth factors are delivered in bound or soluble form. The versatility of the drug delivery system we have developed is apparent in the flexibility of scaffolding material, cell type, and growth factor selection. Thus, the platform can be used to illuminate the delicate balance and roles of growth factors in the complex biological processes that govern tissue and nerve regeneration.

## 2. Materials and Methods

*2.1 Materials and reagents*

Fibrinogen from bovine plasma, thrombin from human plasma, goat serum, poly(ethylene) oxide (PEO, average $M_v \sim 4{,}000{,}000$), lysozyme, accutase, laminin, and epidermal growth factor (EGF), N-Hydroxysuccinimide 98% (NHS) were purchased from Sigma-Aldrich. 1-Ethyl-3-(3-dimetylaminopropyl)carbodiimide (EDC) was purchased from Santa Cruz Biotechnology, Inc.

Glial-derived neurotrophic factor (GDNF) was purchased from PeproTech. Human plasmin was obtained from Athens Research & Technology, Inc. Human neural stem cells were obtained from EMD Millipore. Neurobasal medium, B-27 supplement, N-2 supplement, and basic fibroblast growth factor (bFGF) were purchased from Gibco. Aprotinin was purchased from Quality Biological, Inc. Anhydrous calcium chloride was purchased from Fisher Scientific. CellTracker™ Red CMTPX Dye and alamarBlue® Cell Viability Reagent were purchased from Life Technologies. Rabbit anti-$\beta$III-Tubulin, rabbit anti-GFAP, mouse anti-Nestin, and mouse anti-MAP2 antibodies were purchased from Invitrogen. Cy3 anti-rabbit and Alexa488 anti-mouse were purchased from Jackson ImmunoResearch. Heparin sodium salt from porcine intestinal mucosa was purchased from Calbiochem. Lightning-Link FITC and Lightning-Link Rapid Fluorescein

Antibody Labeling Kits were purchased from Novus Biologicals. Micro-molds were obtained from MicroTissues, Inc.

*2.2 Electrospinning of hydrogel scaffolds*

0.5 wt% fibrinogen was dissolved in 0.2 wt% PEO at 37°C for 20 min, filtered using a 0.2 $\mu$m filter, then placed in a 1 ml syringe fitted with a blunted 27 G needle tip. A 40 ml 50 mM $CaCl_2$ collection solution containing 20 U/ml thrombin was filtered and deposited on a grounded, aluminum collection wheel rotating between 30-40 rpm. The syringe pump holding the spinning solution was programmed to deposit the solution at 3.5 ml/hr. An electrode was attached to the needle tip, the separation distance between the needle tip and the collection wheel was adjusted to approximately 3-3.5 cm from the collection wheel, and an electrical potential of 3.5 kV was applied to the polymer solution. The electrostatically charged polymer jet that formed at the needle tip was ejected into and cross-linked within the rotating collection bath. Scaffolds of fibrin microfibers were formed using a linear stage that rastered the syringe pump back and forth (45-60s for each full pass). The resulting bundle of fibers was given 5 additional minutes after spinning to cross-link further on the wheel. The fibrin sheets were then cut into 7 sections that were each wrapped on square polyethylene terephthalate frames and stored in 12-well plates filled with sterile DI water at 4°C until use.

*2.3 Surface modification of hydrogel scaffolds*

Heparin sodium salt was dissolved in 0.05 M MES to yield a 0.2 wt% solution. EDC and NHS were then added in ratios to heparin of 1:1 and 2:3 by weight, respectively. The solution was mixed for 15 min on a stir plate at room temperature. PBS was then added to yield a solution of 0.1 wt%, which was mixed for an additional 5 min on the stir plate. The activated heparin solution was filtered using a 0.2 $\mu$m filter. Sterile fibrin scaffolds were immediately soaked in the filtered heparin solution for 1 hr at room temperature. Sheets were then washed 3 times for 15 min each in DI water on a shaker at room temperature, then stored in DI water at 4°C until use.

Heparinization was confirmed using 0.1 wt% toluidine blue. Surface modified sheets were soaked in toluidine blue for 20 minutes, then washed 4 times in DI water on a shaker. Positively charged toluidine

blue binds electrostatically to negatively charged heparin, forming a stable, metachromatic heparin-toluidine blue complex.[26] Thus, fibers that remained dark purple after washes indicated presence of heparin.

*2.4 Optimization of factor loading levels in scaffolds*

Modified fibrin scaffolds and unmodified fibrin scaffolds were soaked in 500 ng/ml and 1 $\mu$g/ ml FITC-labeled lysozyme (n=3) overnight at 4°C on a shaker. Lysozyme, approximately 14.3 kDa, was selected for its similar molecular weight to GDNF, approximately 15.1 kDa. Following the overnight soak, sheets were rinsed in PBS for 15 min at 1 ml/ sample on a shaker at room temperature. The solution was collected and replaced with fresh PBS, and the samples were incubated at 37°C. At 3 hr, 6 hr, D1, D3, D5, and D7, release baths were collected and the PBS was replaced. A plate reader was used to read the fluorescence of the release baths (excitation: 485 nm, emission: 528 nm).

Human GDNF was labeled with fluorescein. Modified and control scaffold groups were both loaded at 1 $\mu$g/ ml labeled GDNF (n=3, each). After the overnight growth factor soak, sheets were rinsed in PBS for 15 min at 1 ml/ sample on a shaker at room temperature. The rinse baths were collected and replaced with fresh PBS, and the samples were incubated at 37°C. At 6 hr, D1, D3, D5, D7, D10, and D14, release baths were collected and the PBS was replaced. A plate reader was used to read the fluorescence of the release baths (excitation: 485 nm, emission: 540 nm).

*2.5 NSC culture*

Differentiation media was formed by adding B-27 and N-2 NSC supplements to neurobasal medium. Differentiation media supplemented with 20 $\mu$g/ml bFGF and 20 $\mu$g/ml EGF is referred to as maintenance media.

T75 tissue culture flasks were coated overnight with 20 $\mu$g/ml laminin in 0.9 wt% NaCl. P7 human neural stem cells were plated on laminin-coated T75 flasks, expanded in maintenance media, and cultured in an incubator at 37°C. Media was exchanged every other day, and hNSCs were passaged when confluent. NSCs between passages 8 and 12 were used in experiments.

*2.6 NSC spheroid formation*

Micro-molds were sterilized in 70% ethanol prior to use. 1 wt% agarose was added to 0.9 wt% NaCl, microwaved in increments of 10-15 sec, and swirled until the agarose had fully dissolved. 330 $\mu$l of the agarose solution was pipetted into each micro-mold and allowed to set for 20 min at room temperature. Agarose molds were carefully removed using round tip tweezers and stored in a 24-well plate filled with PBS. PBS was aspirated immediately before use.

hNSCs cultured on T75 flasks were rinsed with PBS twice, then detached using accutase. Cells were spun down at 800 rpm for 4 min. The accutase and media were aspirated, leaving the cell pellet, which was then re-suspended in 500 $\mu$l of NSC maintenance media. 90 $\mu$l of trypan blue was added to 10 $\mu$l of the resuspended cells, and an estimate of the number of the total number of NSCs was calculated based off of the number of stained cells counted in the hemocytometer. The resuspended cells were further diluted down to 50 cells/$\mu$l in maintenance media, and 50 $\mu$l of this dilution was pipetted into each agarose mold to yield approximately 71 cells per spheroid. Spheroids were placed on a shaker in an incubator for 45 min before 500 $\mu$l of maintenance media was added to the sides of each well, carefully avoiding pipetting into the molds. The plates were returned to the shaker at 37°C, and spheroids were given overnight to form.

*2.7 Spheroids culture on tissue culture polystyrene (TCPS)*

All plates used for 2D culture of spheroids on TCPS were coated overnight with 20 $\mu$g/ml laminin in 0.9 wt% NaCl. Prior to use, the laminin solution was aspirated off and maintenance media was added to each well. Spheroids were then added to each well and cultured at 37°C for 7-21 days. Media was exchanged every other day, with fresh GDNF added to experimental groups at specific concentrations.

*2.8 Preparation of scaffolds for spheroid seeding*

Samples were divided into two groups: heparinized scaffolds and nonheparinized scaffolds. Within each group, three loading conditions were used: no GDNF (n=3), bound GDNF (n=3), and soluble GDNF

(n=3). 24 hours prior to spheroid seeding, all samples in the "bound GDNF" groups (heparinized and nonheparinized) were soaked overnight in a GDNF bath to load each sheet with 10 ng/ml GDNF (**Table 1**).

Prior to seeding, all scaffolds were coated with 20 $\mu$g/ml laminin in 0.9 wt% NaCl for 2 hours, then removed from the laminin baths and placed individually into 12-well plates to "dry out" for approximately 20 min before spheroids were added.

| *Type of Microfiber* | *Initial GDNF on Fibers* | *GDNF in Media* | *Fiber Group* |
|---|---|---|---|
| **Nonheparinized** | 0 ng/ml | 0 ng/ml | "No GDNF" |
| **0.1% heparin** | 0 ng/ml | 0 ng/ml | "No GDNF" |
| **Nonheparinized** | 0 ng/ml | 2 or 10 ng/ml | "Soluble GDNF" |
| **0.1% heparin** | 0 ng/ml | 2 or 10 ng/ml | "Soluble GDNF" |
| **Nonheparinized*** | 2 or 10 ng/ml | 0 ng/ml | "Bound GDNF" |
| **0.1% heparin*** | 2 or 10 ng/ml | 0 ng/ml | "Bound GDNF" |

**Table 1.** Loading and culture conditions were categorized into three groups: no GDNF, soluble GDNF, and bound GDNF. *Scaffolds were loaded with 2 or 10 ng/ml GDNF overnight at 4°.

*2.9 Spheroid seeding on scaffolds*

Using round tip tweezers, the agarose molds containing spheroids were flipped such that the bottoms of the molds were facing up. The plates were centrifuged at 400 rpm for 5 min to displace NSC spheroids from the molds. Agarose molds were checked under optical microscopy to ensure they had been emptied, and centrifugation was repeated as necessary. The empty agarose molds were then removed from the plates, and the spheroid suspension was collected from each well. The aggregate spheroid suspension was spun down at 400 rpm for 5 min, and the media was aspirated. The spheroids were resuspended in maintenance media at 20 $\mu$l per mold. Spheroids were seeded onto scaffolds at 10 $\mu$l of spheroid suspension per scaffold, then allowed to attach for 20 minutes before 200 $\mu$l of maintenance media with 10 $\mu$g/ml aprotinin was added carefully to the wells. After an additional hour, the remaining 800 $\mu$l of maintenance media with aprotinin was added to each well to bring the final volume to 1 ml. Aprotinin was added to all media used for culturing NSCs on scaffold in order to prevent fibrinolysis. Samples were cultured at 37°C over the course of 7-21 days depending on the study, and media was exchanged with the respective media conditions every other day. For the "soluble GDNF" condition, 10 ng/ml soluble GDNF was added to maintenance media with aprotinin at each media exchange. For the "no GDNF" and "bound GDNF" conditions, plain maintenance media with aprotinin was added at each exchange.

*2.10 Immunostaining of spheroid-seeded scaffolds*

NSC-seeded scaffolds were rinsed with warm PBS then fixed with 4% PFA for 10 min. Fixed cells were rinsed 3 times in warm PBS, then permeabilized with 0.2% TritonX100 at room temperature. Samples were then washed 5 times with PBS and 0.5% BSA for 5 min each rinse, blocked for 2 hrs with 4% goat serum and 1% BSA in PBS, then washed again 5 times with PBS and 0.5% BSA for 5 min each rinse. For the first set of primary antibody staining, scaffolds were incubated with either rabbit anti-$\beta$III-Tubulin 1:1000 or rabbit anti-GFAP 1:2000 overnight at 4°C. Samples were then washed 5 times with PBS and 0.5% BSA for 5 min each rinse. Shielded from light, scaffolds were incubated with Cy3 anti-rabbit 1:200

for 2 hrs, rinsed 5 times with PBS and 0.5% BSA for 5 min each rinse, then blocked for 2 hrs with 4% goat serum and 1% BSA in PBS. For the second set of primary antibody staining, samples that had been incubated with anti-$\beta$ III-Tubulin previously were incubated with mouse anti-Nestin 1:500 overnight at 4$^{\circ}$ C. Samples that had been incubated with anti-GFAP first were incubated with mouse anti-MAP2 1:500 overnight at 4$^{\circ}$C. Following overnight incubation, all scaffolds were washed 5 times with PBS and 0.5% BSA for 5 min each rinse, Scaffolds were incubated with Alexa488 anti-mouse 1:200 for 2 hrs, then washed 5 times with PBS and 0.5% BSA for 5 min each rinse. Finally, samples were imaged using a Zeiss Axio Observer.A1 microscope.

*2.11 NSC spheroid spreading*

NSCs in monolayer culture on a T75 tissue culture flask were labeled with CellTracker Red prior to spheroid formation as detailed above. Scaffold preparation and spheroid seeding were performed as detailed above, with the addition of a parallel set of all experimental groups cultured in differentiation media with 10 $\mu$g/ml aprotinin rather than maintenance media (n=3 per culture group). Scaffolds were cultured at 37°C for 7 days. Media was exchanged every other day. Scaffolds were imaged daily using fluorescence microscopy. Images were analyzed in ImageJ to quantify outgrowth from spheroids. Spheroids from images taken at 4 hrs, D1, and D2 were outlined and measured using the freeform selection tool. All measurements for a specific time point and culture condition were added together to calculate overall area covered by cells on scaffolds. Changes in overall cell coverage area were calculated relative to spheroid size at 4 hr. At D7, scaffolds were rinsed with warm PBS, then fixed with 4% PFA for 10 min. Fixed cells were stained with Alexa Fluor 488 phalloidin and imaged under fluorescence microscopy using a Zeiss Axio Observer.A1 microscope.

*2.12 NSC spheroid proliferation*

To observe the effects of GDNF on NSC spheroid proliferation, spheroids were seeded on TCPS as described in Section 2.7. At 1.5 hr post-seeding, media was replaced with 10% alamarBlue in maintenance media. After 2.5 hr of incubation, media was collected and absorbance was read using a plate reader (excitation: 540 nm, emission: 590 nm). Maintenance media or GDNF in maintenance media were added.

Spheroids were cultured in the following GDNF concentrations prepared in maintenance media: 0 ng/ml (control), 2 ng/ml, 5 ng/ml, 10 ng/ml, 25 ng/ml, 50 ng/ml GDNF. At D1, D3, D5, and D7, media was replaced with 10% alamarBlue for an incubation time of 2.5 hr before absorbance was read. All remaining media was aspirated, and different conditions of fresh GDNF in media were added to complete the media exchange. Spheroids were rinsed with warm PBS and fixed with 4% PFA at D7.

## 3. Results

*3.1 Heparinization of scaffold surfaces*

EDC was first used to activate the carboxyl groups in heparin and then to react the activated heparin with primary amines on surface of the fibrin fibers. NHS was added to the EDC-heparin solution to stabilize the amine-reactive intermediate, thus increasing the efficiency of the EDC coupling reaction. Fibrin hydrogel microfibers were soaked in this activated heparin solution for 1 hr to allow for surface modification.

Toluidine blue was used to confirm successful functionalization of fibrin scaffolds. Following 20 min of incubation in toluidine blue, excess dye was washed off in a series of soaks in DI. All of the toluidine blue dye that was initially uptaken by unmodified fibers was cleared in the rinses with DI, such that the nonheparinized fibers appeared as they had prior to staining. On the other hand, samples functionalized with 0.1% heparin remained a deep purple color throughout the DI washes. To further confirm heparinization, both groups of fibers were treated with 0.5 CU/ml plasmin at 37°C. Unmodified fibers degraded within 4 hours, while heparinized fibers remained in tact overnight. Heparinized fibers were treated with an additional 0.5 CU/ml plasmin to combat any potential loss of bioactivity of plasmin at 37°C, but no evidence of fiber degradation was observed.

We hypothesized that heparin bound to fibrin shields modified scaffolds from degradation by plasmin. To test this, another group of 0.1% heparinized fibrin scaffolds was incubated with 1 U/ml heparinase overnight at 37°C. After overnight heparinase treatment, modified scaffolds were soaked in 0.5 CU/ml plasmin overnight. Full degradation of fibers following sequential overnight treatments of heparinase and plasmin confirmed our hypothesis. The protection of fibrin by heparin offers great promise for enhancing

stability of fibrin scaffolds when subjected to biologically relevant conditions *in vitro* and eventually *in vivo*.

*3.2 Sustained release of biomolecules bound to surface-modified scaffolds*

Heparinized and nonheparinized fibers were loaded with FITC-labeled lysozyme in soak baths of either 500 ng/ml, 1 $\mu$g/ml or 2 $\mu$g/ml of lysozyme. Lysozyme (14 kDa) was chosen for the initial proof of concept study due to its similar size to growth factors such as GDNF (15 kDa), BDNF (14 kDa), and NGF (13 kDa). The release of lysozyme into PBS at 37°C was recorded over 7 days. Fibers with heparin showed lower release of FITC-lysozyme compared with the release from the nonheparinized control fibers at each time point, indicating capture and prolonged release of FITC-lysozyme from heparinized fibers (**Fig. 1A-C)**. D7 cumulative release from nonheparinized fibers loaded with 500 ng/ml lysozyme was 126.29 ng (86% uptake) compared to 85.36 ng (68.29% uptake) from heparinized fibers loaded with the same initial concentration of lysozyme. At a loading level of 1 $\mu$g/ml lysozyme, cumulative releases of 150 ng (60% uptake) and 103.14 ng (41.26% uptake) were observed in nonheparinized and heparinized fibrin fibers respectively. Cumulative release from nonheparinized fibers loaded with 2 $\mu$g/ml was measured as 356.82 ng (51.36% uptake) and 150. 18 ng (30.04% uptake) from heparinized fibers loaded with 2 $\mu$g/ml (**Table 2**). Percent uptake did not increase with higher loading concentration; however, difference in cumulative release from nonheparinized and heparinized fibers increased by approximately 10% as loading level doubled. Standard deviations also increased monotonically in unmodified fibers. In heparinized fibers, standard deviations from 6 hr until D7 in samples loaded with 2 $\mu$g/ml lysozyme were more than double those in fibers loaded with 500 ng/ml at the same sampling times (**Fig. 1A, C**). In heparinized fibers loaded with 1 $\mu$g/ml lysozyme, standard deviations from release by D1 onward were lower than those for release from fibers loaded with 500 ng/ml lysozyme at corresponding time points. (**Fig. 1B, C**). In the literature, growth factors such as GDNF, VEGF, HGF, and BMP-2 have been found to have higher binding affinity to heparin compared to lysozyme, suggesting that release of these surface-captured factors would be even slower than that of the FITC-lysozyme.[27-30]

The study was repeated with heparinized and nonheparinized fibers loaded overnight with fluorescein-labeled GDNF. Cumulative release at D7 from fibers loaded with 500 ng/ml was approximately 132.14 ng (105.81% uptake) in nonheparinized fibers and about 67.24 ng (53.79% uptake) from heparinized fibers (**Fig. 2A**). Higher cumulative release was observed from heparinized fibers (120.17 ng, 48.07% uptake) compared to nonheparinized fibers (109.06 ng, 43.62% uptake) loaded with 1 $\mu$g/ml GDNF (**Fig 2B**). Finally, a difference of 21.44% in uptake was measured between nonheparinized fibers and heparinized fibers (180.64 ng, 36.23% uptake vs. 73.45 ng, 14.69% uptake) loaded with 2 $\mu$g/ml GDNF (**Fig. 2C**). The percent uptake that surpasses the theoretical loading in the nonheparinized fibers loaded with 500 ng/ml may be attributed to artificial increase in concentration due to evaporation of GDNF release solution collected, particularly at release volumes of 1 ml and at longer time points. Further investigation into fibrin's affinity for GDNF could also potentially explain the observed release. Full degradation of fibers is needed to accurately assess the total amount of growth factor loaded into both heparinized and nonheparinized fibers. We have observed that heparin bound to fibrin protects fibrin from degradation in PBS at 37°C, while unmodified fibers begin fragmenting and appear looser on the frames by D14. Previously, 0.25 CU/ml plasmin was used to degrade nonheparinized fibrin fibers overnight at 37°C (data not shown). However, heparinized fibers remained intact after multiple treatments with plasmin at 37°C. We hypothesize that the high negative charge that heparin imparts to modified fibers protects them degradation via plasmin. Future studies using heparinase to dissociate heparin from fibrin, followed by treatment of the exposed fibrin with plasmin, could provide a means for determining total uptake. Finally, high standard deviations as well as indistinct trends with varying loading concentration may be attributed to degradation of fluorescein. An enzyme linked immunosorbent assay (ELISA) can alternatively be used to measure release and would be particularly useful at later time points since the detection limit of the assay is on the order of picograms.

| *Type of Microfiber Scaffold* | *Initial Concentration of Protein Loaded* | *Percent Uptake of Protein* | *D7 Cumulative Release of Protein* |
|---|---|---|---|
| Nonheparinized | 500 ng/ml lysozyme | 86% | 126.29 ng |
| 0.1% Heparin | 500 ng/ml lysozyme | 68.29% | 85.36 ng |
| Nonheparinized | 1 µg/ml lysozyme | 60% | 150 ng |
| 0.1% Heparin | 1 µg/ml lysozyme | 41.26% | 103.14 ng |
| Nonheparinized | 2 µg/ml lysozyme | 51.36% | 356.82 ng |
| 0.1% Heparin | 2 µg/ml lysozme | 30.04% | 150.18 ng |
| Nonheparinized | 500 ng/ml GDNF | 105.81% | 132.14 ng |
| 0.1% Heparin | 500 ng/ml GDNF | 53.79% | 67.24 ng |
| Nonheparinized | 1 µg/ml GDNF | 43.62% | 109.06 ng |
| 0.1% Heparin | 1 µg/ml GDNF | 48.07% | 120.17 ng |
| Nonheparinized | 2 µg/ml GDNF | 36.23% | 180.64 ng |
| 0.1% Heparin | 2 µg/ml GDNF | 14.69% | 73.45 ng |

**Table 2.** Percent uptake and D7 cumulative release of either FITC-labeled lysozyme or fluorescein-labeled GDNF on nonheparinized and heparinized fibers at varying loading levels. Percent uptake and cumulative release were higher in nonheparinized fibers than in heparinized fibers at all tested loading concentrations of lysozyme. Likewise, percent uptake and cumulative release were both higher in nonheparinized fibers than in heparinized fibers loaded with 500 ng/ml and 2 $\mu$g/ml GDNF. However, greater uptake and release was observed in heparinized fibers loaded with 1 $\mu$g/ml GDNF compared to values from nonheparinized fibers.

**A.**

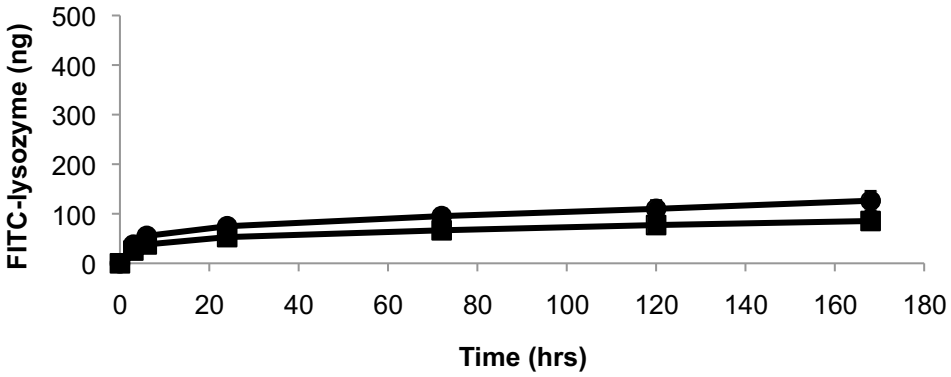


*Release profile of fibrin scaffolds loaded with 500 ng/ml FITC-labeled lysozyme (n=3).*

**B.**

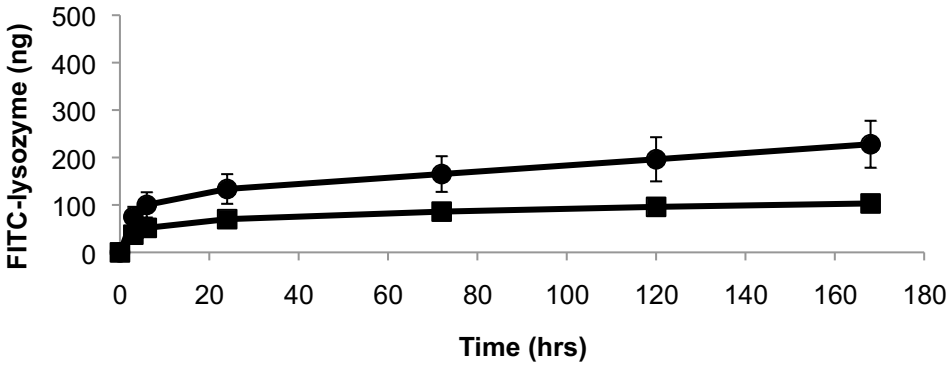


*Release profile of fibrin scaffolds loaded with 1 μg/ml FITC-labeled lysozyme (n=3).*

**C.**

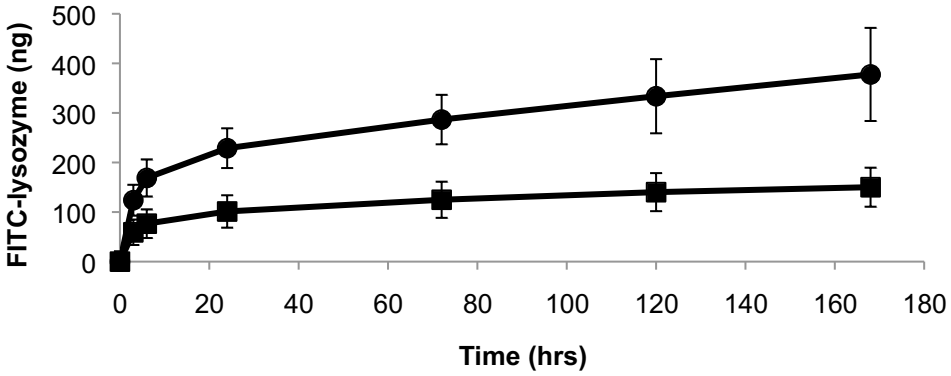


*Release profile of fibrin scaffolds loaded with 2 μg/ml FITC-labeled lysozyme (n=3).*

**Fig. 1.** Cumulative release of FITC-labeled lysozyme from 0.5 wt% fibrin fibers, nonheparinized **(—■—)** vs. modified with 0.1% heparin ( —■— ), over 7 days in PBS at 37°C. Fibers were loaded in overnight baths of **(A)** 500 ng/ml, **(B)** 1 μg/ ml, **(C)** or 2 μg/ ml FITC-labeled lyszoyme. Heparinized fibers showed lower release rates relative to unmodified fibers at all tested loading conditions.

**A.**

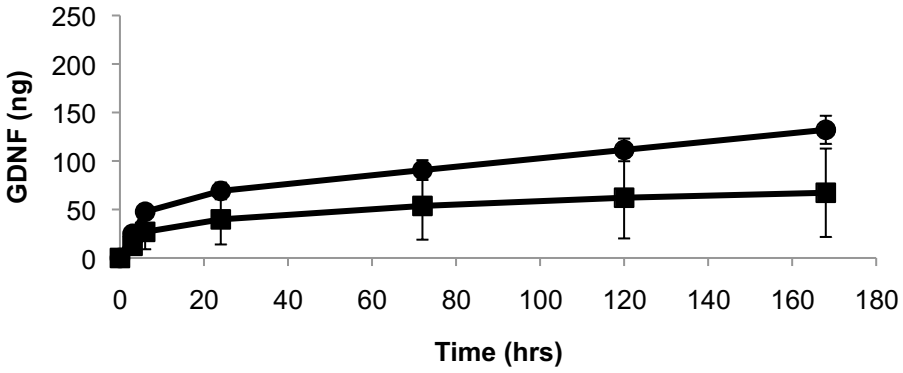


*Release profile of fibrin scaffolds loaded with 500 ng/ml fluorescein-labeled GDNF (n=3).*

**B.**

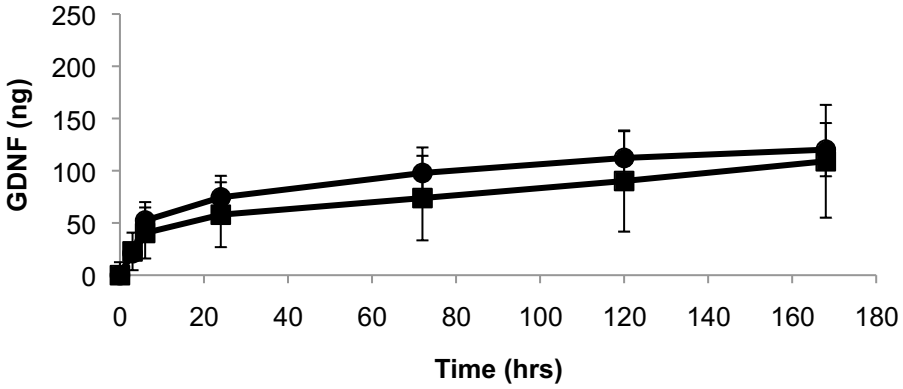


*Release profile of fibrin scaffolds loaded with 1 μg/ml fluorescein-labeled GDNF (n=3).*

**C.**

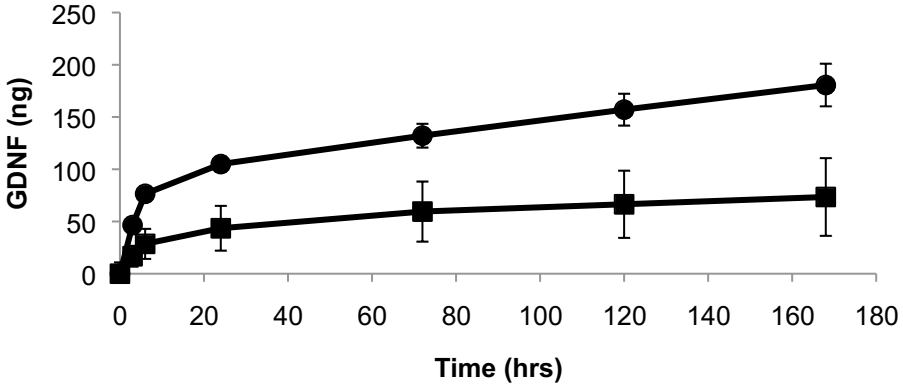


*Release profile of fibrin scaffolds loaded with 2 μg/ml fluorescein-labeled GDNF (n=3).*

**Fig. 2.** Cumulative release of fluorescein-labeled GDNF from 0.5 wt% fibrin fibers, nonheparinized **(—●—)** vs. modified with 0.1% heparin (—■—), over 7 days in PBS at 37°C. Fibers were loaded in overnight baths of (**A**) 500 ng/ml, (**B**) 1 μg/ ml, (**C**) or 2 μg/ ml fluorescein-labeled GDNF. Heparinized fibers show lower release rates relative to unmodified fibers at all tested loading conditions.

*3.3 Effect of GDNF on NSC Proliferation*

NSC spheroids were seeded onto laminin-coated 24-well TCPS plates, then cultured under varying concentrations of GDNF in differentiation media. Metabolic activity of NSCs was measured using alamarBlue, and proliferation was reported relative to the initial metabolic activity of spheroids 4 hours after seeding. At 0, 2, and 5 ng/ml, relative proliferation was consistently lower than the corresponding readings of the 10 ng/ml group at the same time points. Lower proliferation at concentrations higher than 10 ng/ml (25 ng/ml and 50 ng/ml) potentially indicates toxic GDNF dosages. Based on consistently higher relative values of NSC proliferation at each sampling time point, 10 ng/ml was determined to be the optimal concentration for NSC proliferation in differentiation media (**Fig. 3**). Readings of samples cultured with 10 ng/ml soluble GDNF displayed markedly higher proliferation compared to the control group, which was cultured in plain differentiation media, indicating that 10 ng/ml GDNF had a positive proliferative effect on NSCs. 10 ng/ml GDNF was accordingly chosen for subsequent 3D culture of NSC spheroids on electrospun hydrogel fibers.

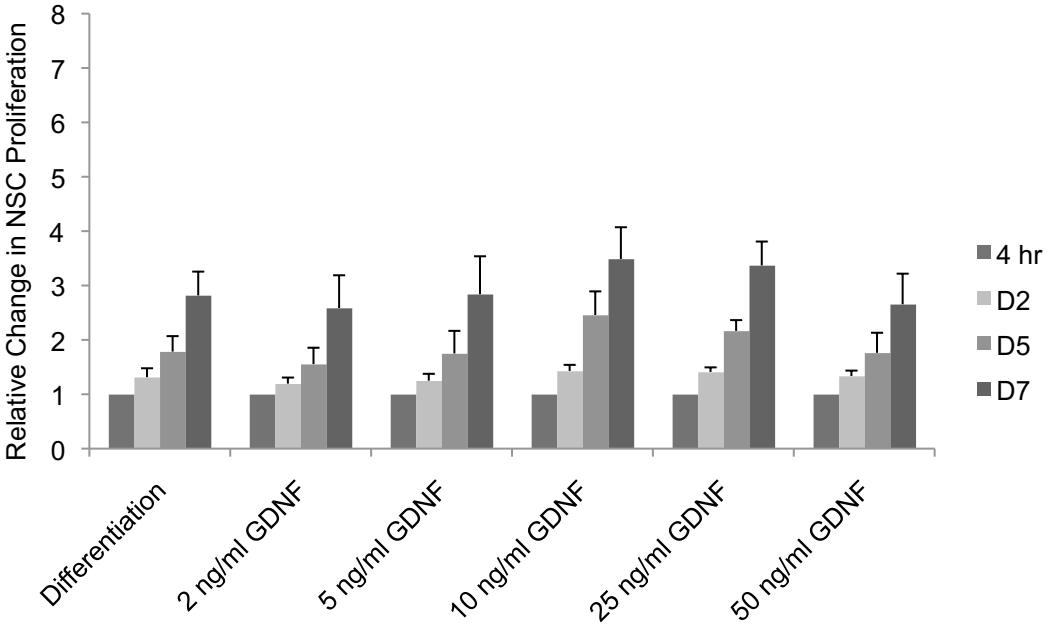


**Fig. 3.** NSC proliferation on TCPS cultured under varying concentrations of GDNF in differentiation media. 10 ng/ml GDNF was determined to be an optimal GDNF concentration for proliferation of NSCs. The greatest differences in proliferation compared to the control (differentiation media only) were observed in NSCs cultured with 10 ng/ml GDNF. Values corresponding to the same time points increased from 2 ng/ml to 10 ng/ml, then decreased again for concentrations above 10 ng/ml.

*3.4 Inhibition of cell outgrowth from spheroids by heparin*

Scaffolds were cultured in maintenance media or differentiation media containing aprotinin, with GDNF immobilized or presented in soluble form in the media. GDNF was delivered either bound to scaffolds (physically entrapped in nonheparinized fibers) or soluble via culture media to determine any differences in presentation and thus release kinetics of GDNF to NSCs. Control scaffolds were cultured in the absence of GDNF. Cell adhesion on scaffolds occurs quickly, and cells were observed growing out from their spheroid conformation and spreading in the orientation of the fibers as early as D1 after seeding onto unmodified fibers. The area covered by cells on unmodified fibers cultured in either maintenance or differentiation media with no GDNF present had more than doubled by D2. By D2 of culture in maintenance media without GDNF, the total area covered by spheroids on heparinized fibers had doubled as well. However, spheroids cultured in differentiation media without GDNF on heparinized fibers had expanded just over 50% after 2 days in culture (**Fig. 4A, Table 3**). Spreading of NSCs on fibers at early time points (4 hr, D1, D2) is of great interest, as rapid cell infiltration into a NGC may maximize the regenerative outcome. Cells that are seeded onto and proliferate on scaffolds prior to implantation can provide their own endogenous cues to enhance regeneration.

Soluble GDNF added to media had a less pronounced effect on cell spreading at early time points overall. After 2 days in culture, cell coverage area on unmodified fibers cultured in maintenance media with 10 ng/ml GDNF had increased by 75.70% and by 67.71% on unmodified fibers cultured in differentiation media with 10 ng/ml GDNF. Cell spreading was again lower on heparinized fibers, with area of spheroid outgrowth increasing by 26.5% when cultured in maintenance media with 10 ng/ml GDNF. Total spheroid area on heparinized fibers cultured in differentiation media with 10 ng/ml GDNF steadily decreased over, falling to 68% of initial spheroid area by D2 of culture (**Fig. 4B, Table 3**). This was the only group in which a decrease in cell spreading was observed.

A final group in which fibers had been loaded with GDNF overnight was studied. We aimed to load 10 ng/ml GDNF into the fibers, as calculated based off of a calibration curve generated previously. Fluorescein labeled-GDNF was loaded into both heparinized and nonheparinized fibers at initial concentrations of 25, 50, 100, 500, and 1000 ng/ml overnight at 4°C. Total GDNF captured by fibers was

measured by fully degrading fibers and measuring the fluorescence of the degradation solution. Unmodified fibers were treated with 0.5 CU/ml plasmin only overnight at 37°C, while heparinized fibers were first soaked in 1 U/ml heparinase overnight at 37°C, followed by another overnight incubation in 0.5 CU/ml plasmin. The cumulative releases at these concentrations was plotted to yield the calibration curve.

A nearly three-fold increase in cell coverage was observed on unmodified fibers soaked overnight in GDNF and cultured in maintenance media for 2 days. Area covered by cells had nearly doubled on unmodified fibers soaked overnight in GDNF and cultured in differentiation media. A sizeable difference was observed between GDNF-bound heparinized fibers that were cultured for 2 days in either maintenance media or differentiation media. Spheroid coverage on heparinized fibers had increased by approximately 131% in maintenance media compared to an increase of approximately 51% in differentiation media (**Fig. 4C, Table 3**).

Beyond D2 of culture, resolution of spheroid spreading became difficult to quantify, particularly on nonheparinized fibers, due to cells coalescing and proliferating along the length of the fibers. At D7, phalloidin staining was used to stain fixed cells for F-actin, a protein essential for important cellular functions such as cell division and migration. Spheroids cultured under all media conditions on nonheparinized fibers displayed significant spreading out of the initial cell aggregates (**Fig. 5**) compared to their heparinized counterparts that remained clustered together, with little outgrowth from their spheroid conformations (**Fig. 5**). However, slight outgrowth was observed from spheroids cultured on heparinized fibers in maintenance media only as well as in differentiation media with 10 ng/ml bound GDNF (**Fig. 5**).

We hypothesize that heparinized fibers bind to the bFGF in maintenance media, thus reducing the maintenance media's ability to facilitate NSC proliferation and outgrowth. The binding of heparin to bFGF in maintenance media effectively transforms maintenance media into differentiation media over time, thus reducing NSC proliferation. Consequently, we reasoned that culture conditions in differentiation media rather than maintenance media were most relevant for studying the effects of GDNF on NSC spreading. Outgrowth from spheroids was observed in all groups of nonheparinized fibers cultured in differentiation media. The area of spreading was greatest when spheroids had been cultured in differentiation media with soluble 10 ng/ml GDNF, slightly lower under culture in differentiation only, and lowest when cultured with 10 ng/ml GDNF entrapped in the scaffolds prior to spheroid seeding. Despite measurements at D1 and D2

indicating an increase in cell coverage on the surfaces of heparinized scaffolds cultured in differentiation media and in differentiation media with 10 ng/ml bound-GDNF, slight outgrowth was only observed from the latter. This suggests that sustained delivery of GDNF over 7 days may have some proliferative effects on NSCs.

Presentation of soluble GDNF was achieved by adding 10 ng/ml fresh to differentiation media with each media exchange every other day. Under these conditions, scaffold area covered by NSC spheroids seeded onto heparinized fibers decreased steadily within the first 2 days of culture, and D7 phalloidin staining showed that cells remained strictly spherical aggregates. A possible explanation for the negative effects on NSC spreading observed in this group may be that the soluble delivery of GDNF at 10 ng/ml may saturate GDNF receptors and ultimately be toxic to NSCs. This hypothesis and the observation of the beginnings of cell outgrowth from spheroids give cause for reversible binding of GDNF using heparin to affect sustained release.

| *Type of Microfiber Scaffold* | *Type of NSC Culture Media* | *GDNF in System* | *Change in Cell Spreading by D2* |
|---|---|---|---|
| Nonheparinized | Maintenance | 0 ng/ml | 154.50% |
| Nonheparinized | Differentiation | 0 ng/ml | 141.48% |
| 0.1% Heparin | Maintenance | 0 ng/ml | 108.76% |
| 0.1% Heparin | Differentiation | 0 ng/ml | 68.73% |
| Nonheparinized | Maintenance | 10 ng/ml (s) | 75.70% |
| Nonheparinized | Differentiation | 10 ng/ml (s) | 67.71% |
| 0.1% Heparin | Maintenance | 10 ng/ml (s) | 26.48% |
| 0.1% Heparin | Differentiation | 10 ng/ml (s) | -32.05% |
| Nonheparinized | Maintenance | 10 ng/ml (b) | 188.40% |
| Nonheparinized | Differentiation | 10 ng/ml (b) | 89.98% |
| 0.1% Heparin | Maintenance | 10 ng/ml (b) | 131.80% |
| 0.1% Heparin | Differentiation | 10 ng/ml (b) | 51.15% |

**Table 3.** Percent change of total scaffold area covered by cells 2 days post-spheroid seeding on scaffolds, relative to area measured at 4 hr. Soluble delivery of GDNF is denoted (s), while presentation of "bound" GDNF is noted with (b). In each delivery group, the greatest amount of early cell spreading was observed on nonheparinized fibers cultured in maintenance media, followed closely by nonheparinized fibers in differentiation media. On heparinized fibers, sustained delivery of GDNF appeared to have an effect on early cell spreading. Proliferation surpassed that of cells on heparinized fibers that were cultured in maintenance media only with no GDNF present. Spreading was lowest across all samples with soluble GDNF delivery of GDNF compared to their "0 ng/ml" and "10 ng/ml (b)" GDNF counterparts.

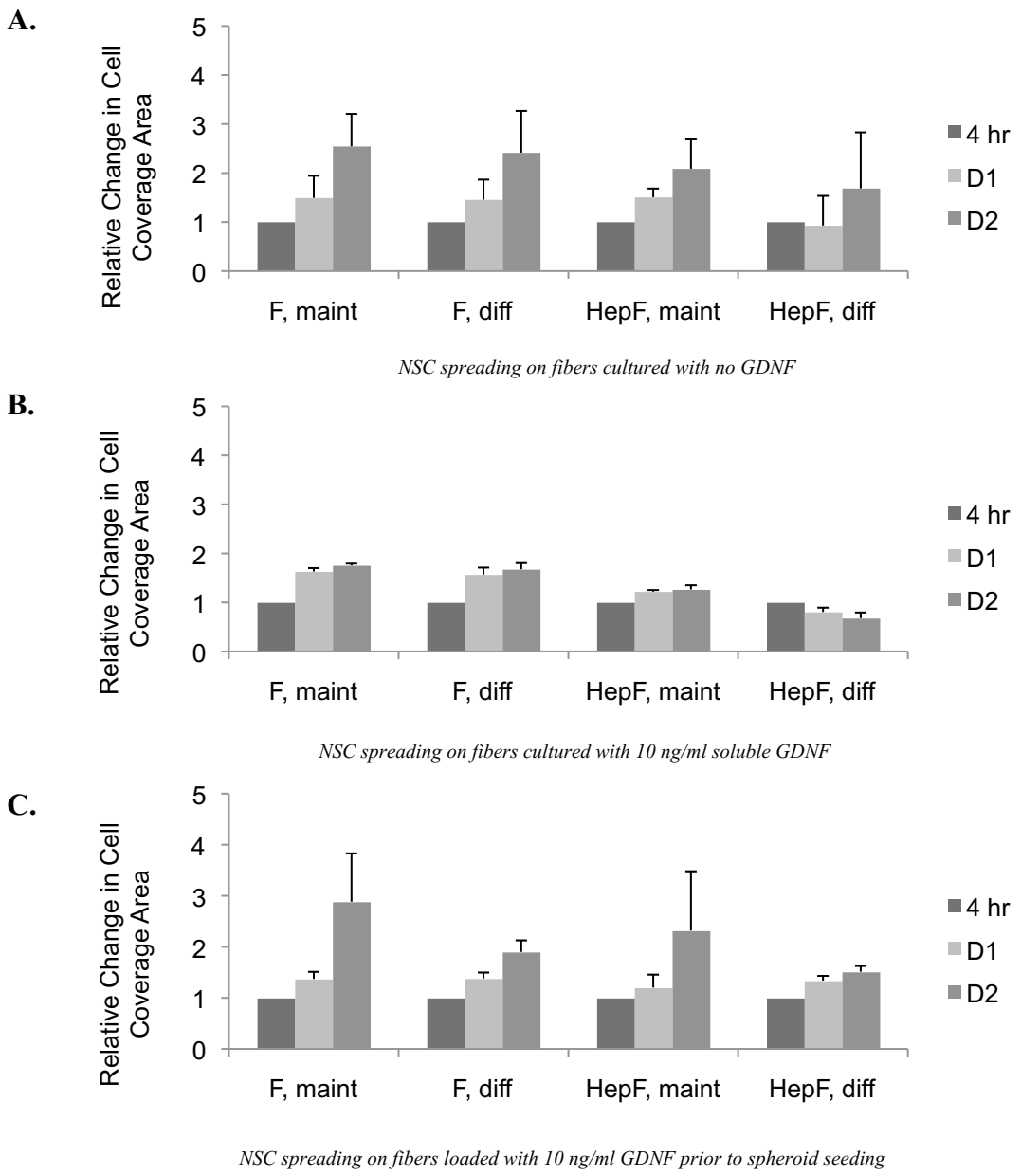


**Fig. 4.** Early outgrowth from NSC spheroids seeded onto nonheparinized and heparinized electrospun hydrogel fibers, measured relative to initial area of spheroid seeding. Cells were cultured on fibers in the presence of no GDNF (**A**), 10 ng/ml soluble GDNF (**B**) , and 10 ng/ml bound GDNF (**C**). Relative changes in cell coverage area were lowest on all fibers when 10 ng/ml soluble GDNF was present. Sustained delivery of GDNF appeared to have a greater proliferative effect on NSCs than soluble delivery of GDNF at early time points.

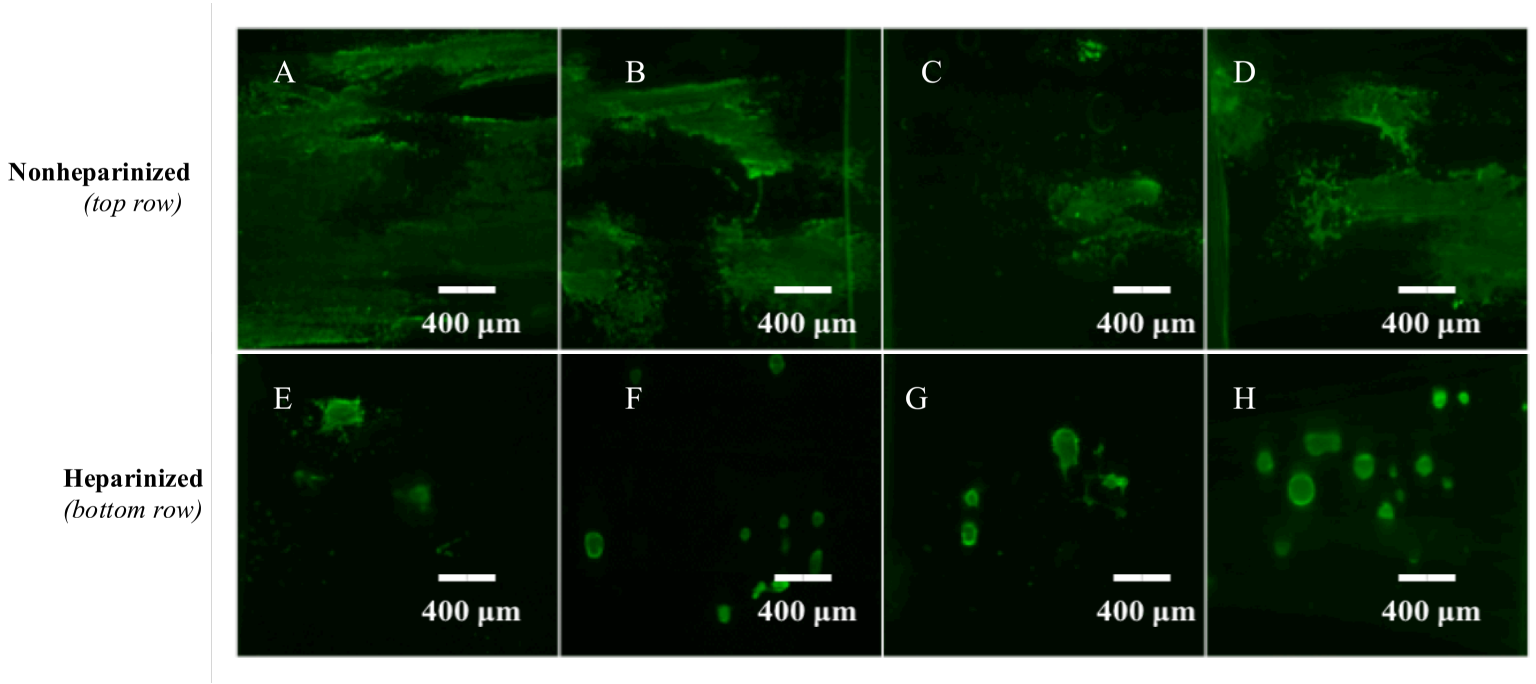


**Fig. 5.** NSC spheroids seeded onto nonheparinized (**A-D**) and heparinized (**E-H**) hydrogel fibers, fixed and phalloidin stained at D7. Spheroids on unmodified fibers were cultured in maintenance media only (**A**), differentiation media and soluble 10 ng/ml GDNF (**B**), differentiation media and bound 10 ng/ml GDNF (**C**), and differentiation media only (**D**). Cell outgrowth and merging of spheroids was observed under all culture conditions on nonheparinized fibers. Cell spreading out from spheroids seeded onto heparinized fibers was also studied under culture in maintenance media only (**E**), differentiation media and soluble 10 ng/ml GDNF (**F**), differentiation media and surface-bound 10 ng/ml GDNF (**G**), and differentiation media only (**H**). Outgrowth was only observed on heparinized fibers cultured in maintenance media and differentiation media + bound 10 ng/ml GDNF.

*3.5 Effect of Heparin on NSC Phenotype and Morphology*

NSC spheroids were seeded onto fibrin hydrogel scaffolds that had either been surface modified with 0.1 wt% heparin or remained untreated. Spheroids were then cultured in differentiation media with no additional growth factors. At D7 and D21, scaffolds were fixed and stained for βIII-tubulin/ nestin and GFAP/MAP2.

Spheroids on nonheparinized fibers had spread out across the length of the fibers by D7, staining positive for both βIII-tubulin and nestin (**Fig. 6A**). However, cells that stained positive for βIII-tubulin only appeared sparingly on the periphery of fibers. By D21, NSCs stained positive for primarily for βIII-tubulin, in high concentration along the edges of the fibers (**Fig. 6B**). MAP2/ GFAP staining did not reveal a dominant phenotype at D7 (**Fig. 6C**), but clear MAP2-positive cells were observed at D21, indicating differentiation of NSCs into neurons (**Fig. 6D**). At D21 in culture, cells cultured on nonheparinized fibers that had degraded appreciably appeared to have remodeled the fibers; neurons appeared in tight, thin bands that were arranged in the orientation of the fibers and spanned the width of each individual remaining fiber respectively. From these results, we conclude that NSCs retain enough stem cell characteristics on nonheparinized fibers at D7 that they generally stain indiscriminately for βIII-tubulin and nestin.

On heparinized fibers, NSCs began spreading out from spheroids following fiber alignment but remained in distinct cell clusters. Staining of D21 samples indicated that some spheroids remained in tact while others had broken apart into individual cells. However, cells from fragmented spheroids had not migrated towards one other to form large patches of cells. A greater portion of cells on heparinized fibers stained positive for βIII-tubulin at D7 (**Fig. 6E**), although there did not appear to be a dominant cell marker at D21 (**Fig. 6F**). MAP2/GFAP staining at D7 indicated the presence of mostly neurons with the appearance of astrocytes on the fringes of spheroids that had begun breaking apart (**Fig. 6G**). Likewise, at D21, cells stained positive for MAP2 and GFAP. GFAP-positive cells were detected solely on the edges of spheroids.

Differentiation media is growth factor-free, no additional growth factors were added to the systems, the fibers were spun under the same conditions, and cells were seeded in an identical manner. Thus, we conclude that heparin inhibits NSC spreading and differentiation, by mechanisms that have yet to be explained.

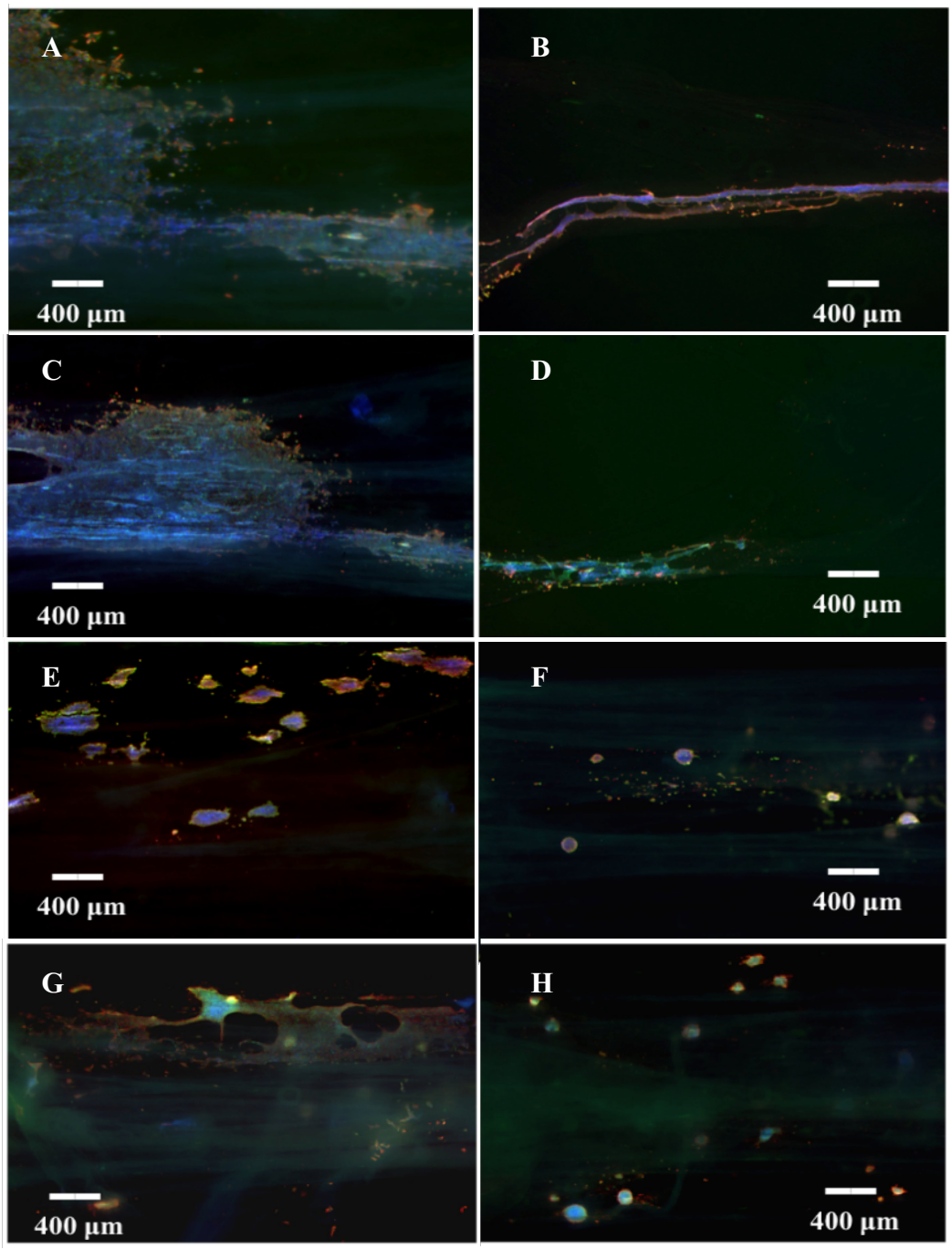


**Fig. 6.** Immunostained NSCs cultured in differentiation media. Spheroids on nonheparinized fibers were fixed and stained for βIII-tubulin (red) and nestin (green) at D7 (**A**) and D21 (**B**), MAP2 (green) and GFAP (red) staining at D7 (**C**) and D21 (**D**). MAP2 stains for dendrites, indicating formation of neurons. βIII-tubulin/ nestin staining of spheroids on heparinized fibers fixed at D7 (**E**) and D21 (**F**). MAP2/GFAP staining on heparinized fibers fixed at D7 (**G**) and D21 (**F**). All samples were DAPI stained (blue).

*3.6 Effects of GDNF on NSC Phenotype and Morphology in 3D Model*

NSC spheroids were seeded onto TCPS and cultured in maintenance and differentiation media under various GDNF conditions, namely 2 ng/ml vs. 10 ng/ml, soluble delivery of factor vs. release of bound factor. Using alamarBlue to quantitatively measure metabolic activity and thus proliferation, we found 10 ng/ml to be an optimal concentration of GDNF in both maintenance and differentiation media for promoting proliferation of NSC spheroids in 2D culture. We then compared the effects of soluble vs. bound delivery of 10 ng/ml of GDNF on NSC spheroids cultured in 3D on fibrin hydrogel microfibers. 2 ng/ml GDNF, the lowest concentration of GDNF that was screened on TCPS, was also studied in the 3D model to determine whether a low level of GDNF would support NSC proliferation and viability. Spheroids cultured on scaffolds were fixed and stained with DAPI, βIII-tubulin/ nestin, and MAP2/GFAP as before.

Nonheparinized fibers stained at D7 did not stain distinguishably for either βIII-tubulin or nestin at D7 (**Fig. 7A**). However, at D21, fewer cells appeared to stain positive for βIII-tubulin compared to cells at D7 (**Fig. 7B**). Additionally, more astrocytes than neurons were observed at D7 (**Fig. 7C**). At D21, it was unclear which phenotype was more prevalent throughout the fibers, as DAPI revealed high confluence of cells spreading out along the entire length and width of nonheparinized fibers, but the ends of the fibers stained positive nearly exclusively for MAP2 (**Fig. 7D**).

Spheroids on heparinized fibers began spreading at D7, and cells stained mostly positive for nestin (**Fig. 7E**). At D21, cells stained positive for βIII-tubulin only on the edges of fibers (**Fig. 7F**). A predominant NSC phenotype was not detected inside the fibers at either D7 (**Fig. 7G**) or D21 (**Fig. 7H**), but the edges of the fibers at both D7 and D21 stained positive for MAP2. DAPI staining also revealed greater outgrowth from spheroids at the later time point.

On nonheparinized fibers cultured in maintenance media and loaded with 2 ng/ml GDNF prior to spheroid seeding, cells had migrated out of spheroids and began proliferating in the orientation of the fibers by D7. Cells at this time point also stained positive for βIII-tubulin on the periphery of nonheparinized fibers (**Fig. 8A**). Distinct areas of spreading and outgrowth from spheroids along the length of the fibers were observed, and MAP2/GFAP staining indicated the presence of astrocytes at D7 as well as some neurons towards the ends of the fibers (**Fig. 8C**). At D21, cells at the edges of the fibers stained positive for nestin and DAPI staining revealed cells having spread out to fill the entire surfaces of fibers (**Fig. 8B**). No

cells were stained due to poor spheroid seeding on nonheparinized D21 samples loaded with 2 ng/ml GDNF overnight.

Heparinized fibers loaded with 10 ng/ml bound GDNF stained positive for both for βIII-tubulin and nestin at D7 (**Fig. 9A**) and D21 (**Fig. 9B**), with no particular preference for either stain. Cells at D7 had migrated out of spheroids, but remained largely separate from one another, whereas by D21, cells had aggregated and were expanding along the fibers. NSCs also almost exclusively stained positive for GFAP at D7 (**Fig. 9C**), indicating formation of astrocytes. MAP2/GFAP staining at D21 revealed several instances of dendrite growth in the same orientation as the microfibers, although the main cell constituents remained astrocytes (**Fig. 9D**).

NSCs appeared to have migrated out of spheroids along the orientation of fibers at D7 on nonheparinized fibers cultured in maintenance media with 10 ng/ml soluble GDNF. Fixed cells stained positive for βIII-tubulin at the ends of and nestin towards the centers of the fibers (**Fig. 10A**), as well as for GFAP (**Fig. 10C**) at D7. DAPI staining revealed cells had proliferated across the entirety of fiber surfaces at D21. Cells stained positive for both βIII-tubulin and nestin on fibers at D21 (**Fig. 10B**). MAP2 positive cells were detected across all remaining sections of fiber that had not degraded by D21, indicating the presence of neurons that had grown outwards in bands in the direction of the fibers (**Fig. 10D**).

Cells that were initially seeded as spheroids on heparinized fibers and exposed to 10 ng/ml soluble GDNF in maintenance media had largely migrated out by D7, although distinct patches of cells were still recorded. Cells stained positive for nestin, and minimal βIII-tubulin was detected at D7. Staining with DAPI also revealed cells growing in the direction of the fibers (**Fig. 10E**). No cells stained positive for MAP2 at D7 (**Fig. 10G**). At D21, staining still exposed several areas where spheroids had expanded in the direction of the fibers yet remained separate from other spheroids. More cells staining positive for βIII-tubulin were detected, and with almost all βIII-tubulin stained cells appearing on the edges of the fibers. D21 DAPI staining also revealed a clear preferential direction of cell growth along the length of the fibers (**Fig. 10F**). Large areas of GFAP positive cells were observed at D21, and MAP2 was also detected in faint bands in the direction of the fibers (**Fig. 10H**).

Immunostaining of samples fixed at D21 revealed that the presence of heparin inhibited cells from spreading out from the initial aggregates under culture in maintenance media only as well as in differentiation media only. However, in general, when GDNF was present in culture, spheroids appeared to be able to spread out on the heparinized fibers to a greater extent. Samples cultured with 10 ng/ml bound GDNF in maintenance media did not stain positive for cells, indicating poor spheroid seeding in this group. 10 ng/ml GDNF was previously shown in 2D culture to be an optimal concentration for promoting NSC proliferation.

Cells on unmodified fibers after D7 of culture with 2 ng/ml soluble GDNF stained positive for both βIII-tubulin/ nestin, with a greater concentration of βIII-tubulin positive cells. Cells of the 2 ng/ml "bound" GDNF delivery group on nonheparinized fibers at D7 stained positive largely for βIII-tubulin. However, D21 βIII-tubulin/ nestin staining of samples from both groups of 2 ng/ml GDNF delivery indicated a greater concentration of cells that stained positive for nestin, an early neural stem cell marker, rather than βIII-tubulin, a neuronal marker. Cell spreading was unaffected in either group. This unexpected result may indicate that 2 ng/ml GDNF is an insufficient dosage of GDNF to significantly influence neuronal differentiation on nonheparinized fibers. On the other hand, at D21, cells stained positive exclusively for MAP2 on nonheparinized fibers cultured with 10 ng/ml soluble GDNF, with no indication of the presence of astrocytes, suggesting target delivery of 10 ng/ml GDNF to NSCs cultured in a 3D model may enhance and direct neuronal outgrowth.

On heparinized fibers, all groups stained positive for nestin at D7, and concentrated areas of cells cultured with 10 ng/ml soluble GDNF and in differentiation media only also stained positive for βIII-tubulin. At D21, all samples stained either a comparable or noticeably lower degree for nestin. Samples of the groups cultured in maintenance media only and with 2 ng/ml soluble GDNF stained positive almost entirely for βIII-tubulin. A lack of pronounced difference in differentiation between samples treated with 2 ng/ ml GDNF and with 10 ng/ml GDNF may be due to the presence of heparin sequestering growth factors released by the cells endogenously as well as GDNF, bFGF, and EGF delivered in culture, consequently playing an undetermined role in the promotion or inhibition of NSC differentiation.

The greatest concentration of cells that stained positive for GFAP, an astrocytic marker, appeared on the edges of fibers on which NSCs had migrated out of spheroids as well as outlining spheroids that remained in tact regardless of degree of heparinization of the scaffold surfaces. On unmodified fibers, cells stained positive for GFAP at varying degrees under all culture conditions, although cells cultured in maintenance media only and in differentiation media only stained predominantly for MAP2 at D7. By D21, GFAP staining was minimal in nearly all unmodified fibers, with the exception of the 2 ng/ml soluble GDNF delivery group, in which cells on the edges of the fiber stained positive for GFAP. However, cells cultured on heparinized fibers under all culture conditions, regardless of delivery method and concentration of GDNF, stained positive for both astrocytes and neurons even at D21. The observation of concentrated areas of cells that stained positive for GFAP at D21 on heparinized fibers but not on nonheparinized fibers may suggest that the presence of heparin, via recruitment and release of neurotrophic factors, plays a role in influencing cell lineage as NSCs differentiate. As astrocytes are closely associated with neuronal synapses and provide metabolic support to neurons, the ability to sustain both phenotypes in culture can potentially be exploited for applications in treatment of neurodegenerative diseases and disorders.

A direct comparison of NSCs cultured on unmodified fibers cultured in differentiation media with soluble growth factor and NSCs seeded onto heparinized fibers with bound growth factors in differentiation media would provide insight into how soluble and sustained delivery of biochemical cues independently affect differentiation and cell phenotype. Maintenance media was used in this study to promote cell proliferation, but bFGF and EGF in the media may bind to heparin or play an undetermined synergistic or competitive role when GDNF is present in the system. Growth factors secreted by NSCs may also bind to and be subsequently released by heparin at a later time point. Culturing NSCs on fibers in differentiation media, where the only exogenous growth factor present is GDNF, would provide a means of studying the effect of GDNF on NSC proliferation and phenotype via culture on unmodified fibers. Through close study of the saturation levels of growth factors bound to heparin, we can tune the degree of heparinization so as to minimize free heparin groups to which endogenous growth factors released post-cell seeding can bind to and potentially mute any effects of GDNF on cellular response. Additionally, lack of cells on several heparinized fiber groups indicates a need for improving cell adhesion when scaffold surfaces have been modified. A sandwich configuration that consists of a middle heparinized layer with bound growth factors

wrapped in unmodified fibers onto which spheroids would be seeded is proposed and will be evaluated in future studies.

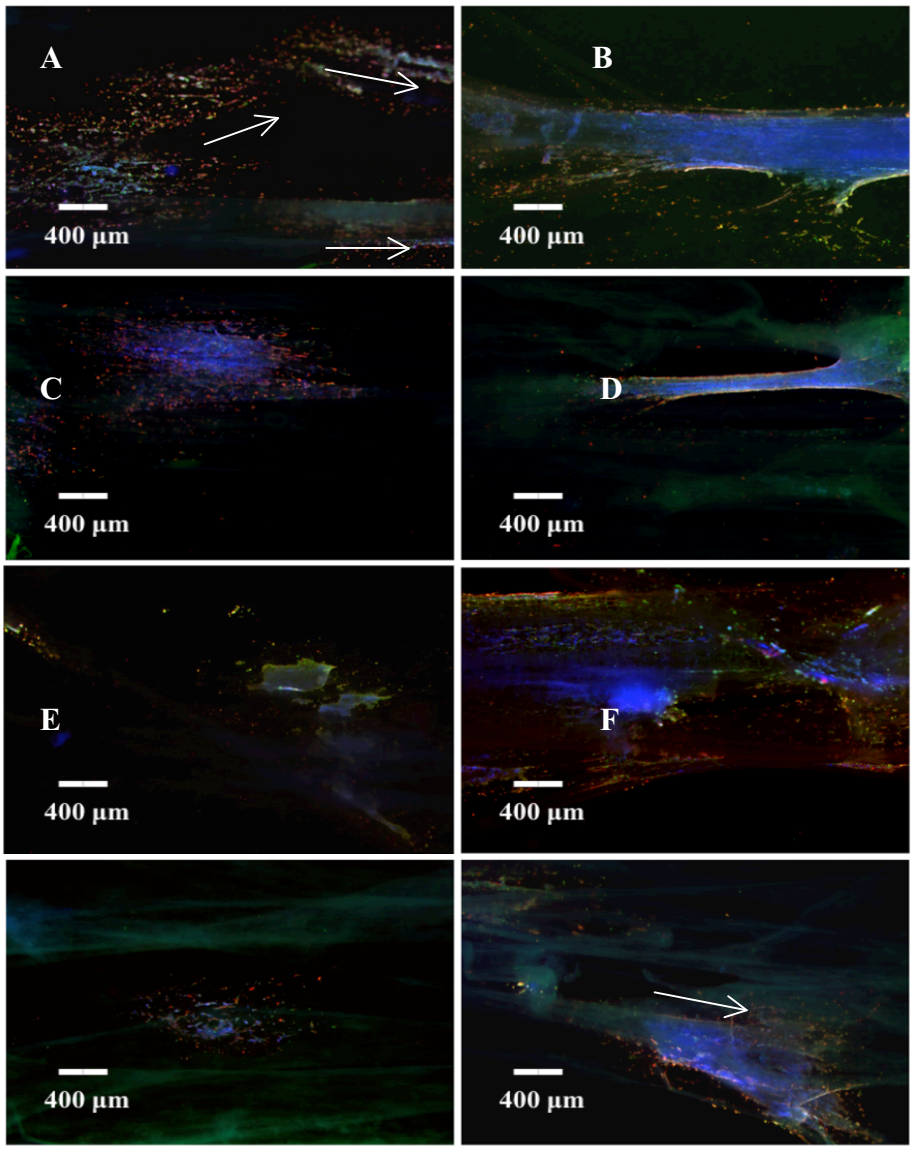


**Fig. 7.** Immunostained NSCs on nonheparinized (**A-D**) and heparinized (**E-H**) fibers loaded with 2 ng/ml soluble GDNF in maintenance media. Spheroids on nonheparinized fibers were fixed and stained for βIII-tubulin/ nestin at D7 (**A**) and D21 (**B**). MAP2/GFAP staining revealed differences in NSC phenotype at D7 (**C**) and D21 (**D**). Heparinized fibers were stained for βIII-tubulin/ nestin at D7 (**E**) and D21 (**F**), as well as MAP2/GFAP at D7 (**G**) and D21 (**H**). On nonheparinized fibers, cells stained positive for both βIII-tubulin and nestin at D7 and D21. More cells stained positive for GFAP at D7 and for MAP2 at D21. Cells on the edges of heparinized fibers stained positive for βIII-tubulin at D21. Both GFAP and MAP2 positive cells were observed at D21 on heparinized fibers. All fibers were stained with DAPI.

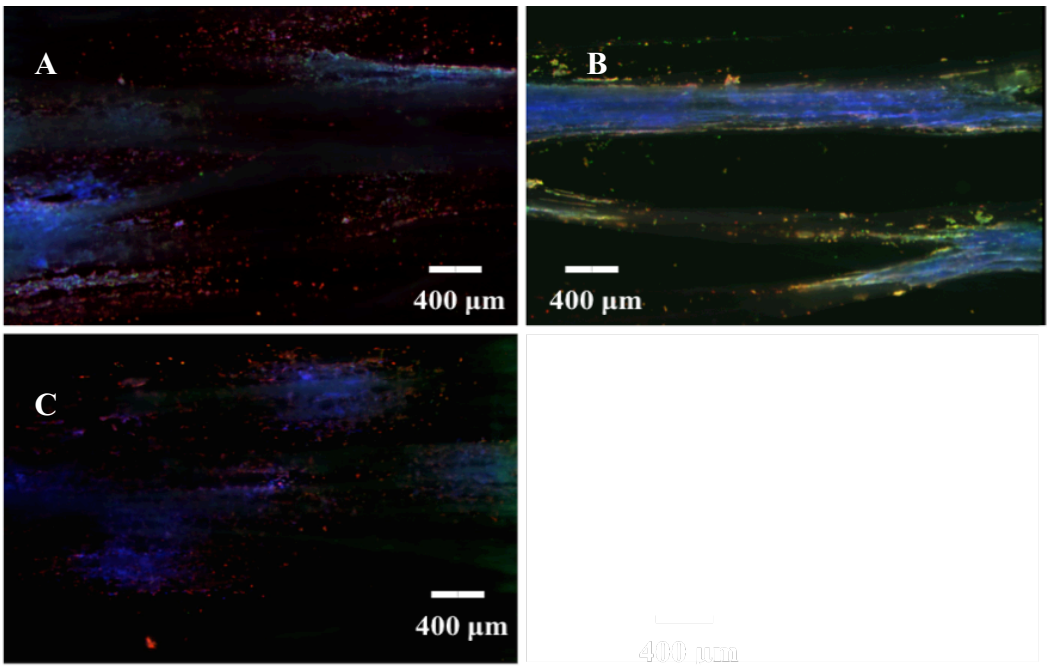


**Fig. 8.** Immunostained NSCs on nonheparinized fibers loaded with 2 ng/ml bound GDNF and cultured in maintenance media. All samples were stained with DAPI. Spheroids on nonheparinized fibers were fixed and stained for βIII-tubulin/ nestin at D7 (**A**) and D21 (**B**). Fixed spheroids were also stained for MAP2/GFAP at D7 (**C**). Cells stained positive for βIII-tubulin and MAP2 at D7. At D21, cells stained positive for predominately nestin. MAP2/GFAP staining at D21 revealed no cells, which can be attributed to poor cell seeding, and thus are not pictured.

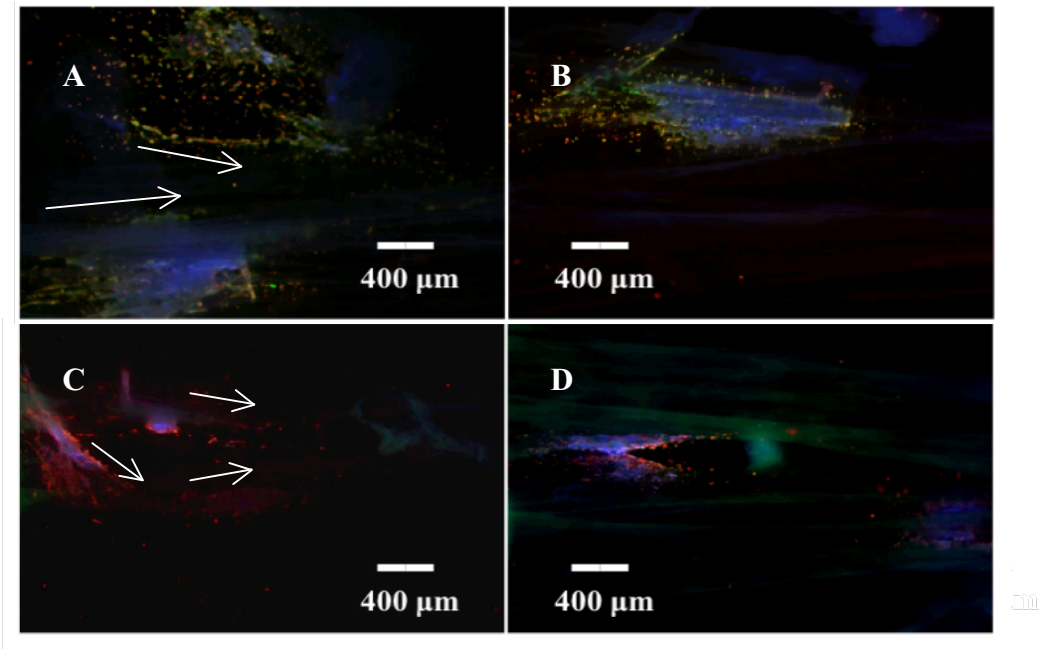


**Fig. 9.** Immunostained NSCs on heparinized fibers loaded with 2 ng/ml bound GDNF were stained for βIII-tubulin/ nestin at D7 (**A**) and D21 (**B**), as well as MAP2/GFAP at D7 (**C**) and D21 (**D**). All samples were stained with DAPI. Cells had migrated out of spheroids but remained separate from one another by D7. At D7, cells stained positive for both βIII-tubulin and nestin at D7 and almost exclusively for GFAP, indicating presence of astrocytes. NSCs had aggregated and grown following the direction of fibers by D21. Cells fixed at this time point stained positive for both βIII-tubulin and nestin, as well as for both GFAP (fibers in focus) and MAP2 (fibers out of focus).

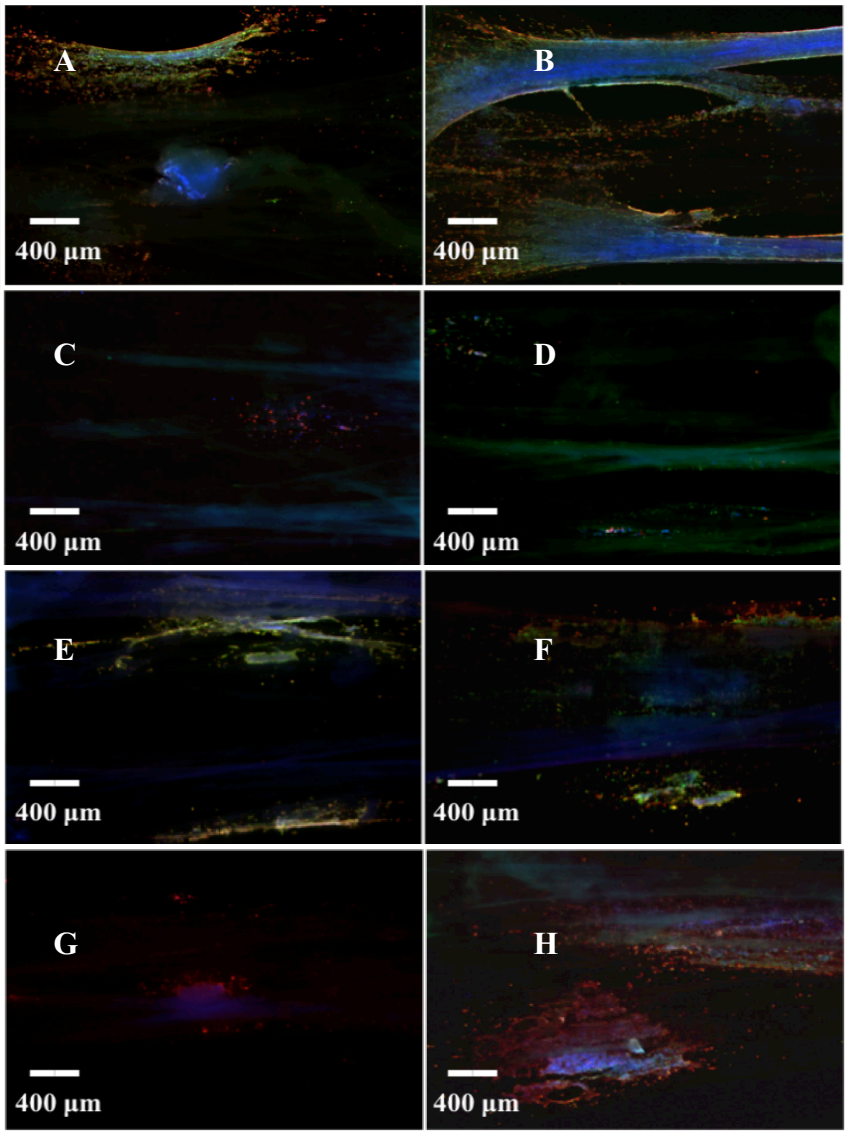


**Fig. 10.** Fixed and immunostained NSCs on nonheparinized (**A-D**) and heparinized (**E-H**) fibers cultured in maintenance media with 10 ng/ml soluble GDNF. All samples were stained with DAPI. Cells on nonheparinized fibers were stained for βIII-tubulin/ nestin at D7 (**A**) and D21 (**B**), as well as MAP2/GFAP at D7 (**C**) and D21 (**D**). Cells on heparinized fibers were stained for βIII-tubulin/ nestin at D7 (**E**) and D21 (**F**), as well as MAP2/GFAP at D7 (**G**) and D21 (**H**). On nonheparinized fibers, cells stained positive for GFAP only at D7 and MAP2 only at D21. On heparinized fibers, cells had largely migrated out of spheroids by D7, although distinct patches of cells were still observed at D21. Cells stained positive primarily for nestin at D7 and both nestin and βIII-tubulin (on the edges of fibers) at D21. Both GFAP and MAP2 positive cells were observed at D21.

## 4. Discussion

We report a simple, scalable platform for capturing growth factors on the surface of aligned, hydrogel fibers using heparin. Fibrin scaffolds were selected for this study, but the EDC/NHS coupling of heparin employed affords great flexibility to the system in that any biopolymer hydrogel containing primary amines, or carboxylic acid groups when a diamine linker is used, can be functionalized. The utility of this surface conjugation method is further extended by the large number of growth factors that contain heparin-binding domains and can thus be studied in the context of specific regenerative medicine applications.

We demonstrated sustained release of FITC-lysozyme as well as GDNF from heparin-conjugated fibrin hydrogel microfibers. Percent of heparinization is defined as weight of heparin dissolved per volume of final soak solution (w/v), which consisted of a 1:1 ratio of 0.05 MES buffer to PBS. Thus, the concentration of the heparin soak bath can be easily tuned. While changes in percent heparinization would also require tuning of factor uptake and release, this could be useful if a greater number of free heparin groups on fiber scaffolds or different release kinetics for the delivery of growth factor(s) beyond GDNF were sought.

NSCs on nonheparinized fibers migrated out of spheroids quickly after seeding and continued to grow in the direction of the fibers. Heparin appeared to inhibit spreading of neural stem cells out of spheroids on hydrogel scaffolds in the absence of any growth factors. This suggests heparin binds to either NSC surfaces or endogenous growth factors released by NSCs, thus restricting the transmission of biochemical cues to signal outgrowth from spheroids across fiber surfaces. However, the presence of GDNF in culture on heparinized fibers appeared to supersede the inhibitory effects of heparin alone on cell spreading.

Notably, NSC phenotype differed significantly on heparinized and nonheparinized fibers for all conditions of GDNF, regardless of concentration or delivery method. Cells on nonheparinized fibers stained positive exclusively for neurons, whereas all heparinized samples stained positive for both astrocytes and neurons. Although the precise role of astrocytes in the neurodegenerative diseases remains unclear, there are many indications of mechanisms by which astrocytes support neurons in the normal brain. In the literature, neurons co-cultured with astrocytes have exhibited higher levels of glutathione, an antioxidant that prevents damage to cellular components, compared to neurons cultured alone.[31, 32] Likewise, astrocytes take up glutamate and convert it into glutamine, which is released to the extracellular

space where it is taken up by neurons. Neurons then use glutamine to synthesize glutamate in order to replenish the neurotransmitter pool. Astrocytes also regulate neuronal activation by extracellular potassium uptake and help maintain ion gradients. As astrocytes upregulate glucose transporters to provide energy to dying neuronal cells, they are believed to play a crucial role in the improvement of energy metabolism in chronic neurodegenerative diseases.[33]

Astrocyte functions vary with respect to specific neurodegenerative diseases. For example, in Alzheimer's disease (AD), astrocytes accumulate neuron-derived amyloid material that results from local neurodegeneration. $GFAP^+$ amyloid plaques then form when astrocytes undergo cell death as a result of substantial neurodegenerative debris accumulation. The disease process also increases calcium signaling between astrocytes, which is believed to contribute to the dysfunction or death of neurons.[34-37] Preservation of astrocyte function is thus a keystone goal against AD. In Parkinson's disease (PD), the second most prevalent neurodegenerative disease after AD, emphasis is shifting from studying the loss of dopaminergic neurons and depletion of dopamine to understanding the role nonneuronal cells play in producing neuroprotective functions in PD. Exposure of astrocytes to nitric oxide increases glutathione production by astrocytes. Increased availability of glutathione to neurons in turn makes neurons less susceptible to reactive nitrogen species. In PD patients, glutathione-containing cells have been found in regions with preserved dopaminergic neurons, further supporting the theory that astrocytes serve a neuroprotective purpose in PD.[38]

Contrarily, astrocyte involvement in neurodegenerative contexts has also been observed. In amyotrophic lateral syndrome (ALS) patients, increased astrocyte activation and expression of inflammatory markers are established hallmarks of ALS disease progression.[39, 40] Likewise, exposure of astrocytes in multiple sclerosis (MS) plaques to inflammatory cytokines has been shown to trigger unregulated inflammatory responses. Increased noradrenalin levels leads to axonal and myelin damage in MS patients.[41, 42]

Overall, the neurodegenerative and neuroprotective mechanisms astrocytes are involved in indicate that modulating astrocyte function may be an important consideration in developing successful therapeutic strategies in the treatment of neurodegenerative disorders.[43] The results from our study indicate a phenotypic distinction in differentiated NSCs cultured on heparinized vs. nonheparinized fibers, suggesting

that in addition to providing topographic and biochemical cues to enhance cell survival, our surface-modified fibers can potentially influence stem cell differentiation. Individual aspects of the platform proposed, such as materials selection, degree of heparinization, release kinetics, and growth factors to be delivered, can all be tuned in order to gain a deeper understanding of specific pathological states and subsequently design therapeutic treatments to combat these diseases.

## 5. Conclusion

The utility of hydrogel microfibers is significantly improved by conjugating heparin to the surfaces of these fibers, thereby providing a means for binding and controlling the release kinetics of growth factors *in vitro*. The method of heparinization used can easily be scaled up or down, and selection of biochemical cues is only limited by the lack of heparin-binding site on the growth factors themselves. Due to the post-electrospinning modification of the fibers using heparin, structural integrity and cross-linking of the hydrogel fibers is not compromised by the addition of heparin, and a wide range of biopolymers can be used in scaffold formation.

Fibrin fibers modified with heparin to bind GDNF displayed lower release rates relative to those of unmodified fibers loaded at the same concentration, indicating capture and sustained release of GDNF. Due to its high negative charge, heparin appears to protect fibers from degradation by plasmin delivered exogenously in acellular studies and proteases secreted by NSCs. Immunostaining revealed that heparin alone inhibited spreading of NSCs out of spheroids seeded onto scaffolds, but the presence of GDNF seemed to override these inhibitory effects to enhance cell outgrowth. Finally, a phenotypic difference was observed in preliminary cell studies: unmodified fibers stained positive nearly exclusively for neurons, while heparinized samples stained positive for both astrocytes and neurons.

Prolonged release of GDNF, protection of underlying fibrin scaffolds, and influence over NSC phenotype were achieved using heparin conjugated to the surface of fibrin hydrogel microfibers. NSCs, GDNF, and fibrin were selected for the preliminary cell culture study, but there are few restrictions on cell line, growth factor(s), and scaffold biopolymer. Thus, the versatility and ease of adaptability of this

heparin-based system make it a promising therapeutic strategy for studying a host of neurodegenerative disorders.

## 6. References


[1] Feinberg AW. Engineered Tissue Grafts: Opportunities and Challenges in Regenerative Medicine. WIREs Syst Biol Med 2012;4:207–220.

[2] Heath, CA, Rutkowski GE. The Development of Bioartificial Nerve Grafts for Peripheral-nerve Regeneration. Trends in Biotechnology 1997;16:163-68.

[3] Serban MA, Prestwich GD. Modular Extracellular Matrices: Solutions for the Puzzle. Methods 2008;45:93-98.

[4] Liu H, Zhou Y, Chen S, Bu M, Xin J, Li S. Current Sustained Delivery Strategies for the Design of Local Neurotrophic Factors in Treatment of Neurological Disorders. Asian Journal of Pharmaceutical Sciences 2013;8:269-77.

[5] Huang YC, Huang YY. Biomaterials and Strategies for Nerve Regeneration. Artificial Organs 2006;30:514-22.

[6] Dodla MC, Mumaw J, Stice SL. Role of Astrocytes, Soluble Factors, Cells Adhesion Molecules and Neurotrophins in Functional Synapse Formation: Implications for Human Embryonic Stem Cell Derived Neurons. CSCR Current Stem Cell Research & Therapy 2010;5:251-60.

[7] Chan BP, Leong KW. Scaffolding in Tissue Engineering: General Approaches and Tissue-specific Considerations. European Spine Journal Eur Spine J 2008;17:467-79.

[8] Szentivanyi A, Chakradeo T, Zernetsch H, Glasmacher B. Electrospun Cellular Microenvironments: Understanding Controlled Release and Scaffold Structure. Advanced Drug Delivery Reviews 2011;63:209-20.

[9] Braghirolli, DI, Steffens D, Pranke P. Electrospinning for Regenerative Medicine: A Review of the Main Topics. Drug Discovery Today 2014;19:743-53.

[10] Zhang S, Liu X, Barreto-Ortiz SF, Yu Y, Ginn BP, Desantis NA, et al. Creating Polymer Hydrogel Microfibres with Internal Alignment via Electrical and Mechanical Stretching. Biomaterials 2014;35:3243-251.

[11] Straley KS, Foo CWP, Heilshorn SC. Biomaterial Design Strategies for the Treatment of Spinal Cord Injuries. Journal of Neurotrauma 2010;27:1-19.

[12] Ji W, Sun Y, Yang F, van den Beucken JJJP, Fan M, Chen Z, et al. Bioactive Electrospun Scaffolds Delivering Growth Factors and Genes for Tissue Engineering Applications. Pharm Res Pharmaceutical Research 2011;28:1259-272.

[13] Zhao, H, Ma L, Zhou J, Mao Z, Gao C, Shen J. Fabrication and Physical and Biological Properties of Fibrin Gel Derived from Human Plasma. Biomed. Mater. Biomedical Materials 2007;3:015001.

[14] Ahmed, GAE, Dare EV, Hincke M. Fibrin: A Versatile Scaffold for Tissue Engineering Applications. Tissue Engineering Part B: Reviews 2008;14:199-215.

[15] Domb AJ, Kumar N, Ezra A. Tissue Engineering. Biodegradable Polymers in Clinical Use and Clinical Development. Wiley 2011.

[16] Shastri VP, Altankov G, Lendlein A. Nanocomposities for Regenerative Medicine. Advances in Regenerative Medicine Role of Nanotechnology and Engineering Principles : Proceedings of the NATO Advanced Research Workshop on Nanoengineered Systems for Regenerative Medicine Varna, Bulgaria 21-24 September 2007. Springer 2010;192-3.

[17] Reed S, Wu B. Sustained Growth Factor Delivery in Tissue Engineering Applications. Annals of Biomedical Engineering Ann Biomed Eng 2013;42:1528-536.

[18] Ramburrun P, Kumar P, Choonara YE, Bijukumar D, Du Toit LC, Pillay V. A Review of Bioactive Release from Nerve Conduits as a Neurotherapeutic Strategy for Neuronal Growth in Peripheral Nerve Injury. BioMed Research International 2014;1-19.

[19] Sakiyama-Elbert SE. Incorporation of heparin into biomaterials. Acta Biomater 2013;10:1581-7.

[20] Sakiyama-Elbert SE, Hubbell JA. Controlled Release of Nerve Growth Factor from a Heparin-containing Fibrin-based Cell Ingrowth Matrix. Journal of Controlled Release 2000;69:149-58.

[21] Taylor SJ, Mcdonald III JW, Sakiyama-Elbert SE. Controlled Release of Neurotrophin-3 from Fibrin Gels for Spinal Cord Injury. Journal of Controlled Release 2004;98:281-94.

[22] Jandik KA, Kruep D, Cartier M, Linhardt RJ. Accelerated Stability Studies of Heparin. Journal of Pharmaceutical Sciences J. Pharm. Sci. 1996;85:45-51.

[23] Olwin BB. Heparin-binding Growth Factors. Cytotechnology 1989;2:351-65.

[24] Thorne RG, Frey II WH. Delivery of Neurotrophic Factors to the Central Nervous System. Clinical Pharmacokinetics 2011;40:907-46.

[25] Vishwakarma SK, Bardia A, Tiwari SK, Paspala SAB, Khan AA. Current Concept in Neural Regeneration Research: NSCs Isolation, Characterization and Transplantation in Various Neurodegenerative Diseases and Stroke: A Review. Journal of Advanced Research 2014;5:277-94.

[26] Peng XY, Luo HQ, Li NB. Voltammetric Study on the Interaction of Heparin with Toluidine Blue, and Its Analytical Application. Microchimica Acta Microchim Acta 2006;156:297-302.

[27] Roam JL, Nguyen PK, Elbert DL. Controlled Release and Gradient Formation of Human Glial-cell Derived Neurotrophic Factor from Heparinated Poly(ethylene Glycol) Microsphere-based Scaffolds. Biomaterials 2014;35:6473-481.

[28] Zhao W, Mccallum SA, Xiao Z, Zhang F, Linhardt RJ. Binding Affinities of Vascular Endothelial Growth Factor (VEGF) for Heparin-derived Oligosaccharides. Bioscience Reports Biosci. Rep. 2011;32:71-81.

[29] Barnett MW, Fisher CE, Perona-Wright G, Davies JA. Signalling by Glial Cell Line-derived Neurotrophic Factor (GDNF) Requires Heparan Sulphate Glycosaminoglycan. Journal of Cell Science 2002;115:4495-503.

[30] Ruppert R, Hoffmann E, Sebald W. Human Bone Morphogenetic Protein 2 Contains a Heparin-Binding Site Which Modifies Its Biological Activity. Eur J Biochem European Journal of Biochemistry 1996;237:295-302.

[31] Slemmer JE, Shacka JJ, Sweeney MI, Weber JT. Antioxidants and free radical scavengers for the treatment of stroke, traumatic brain injury and aging. Curr Med Chem 2008;15:404-414.

[32] Giordano G, Kavanagh TJ, Costa LG. Mouse cerebellar astrocytes protect cerebellar granule neurons against toxicity of the polybrominated diphenyl ether (PBDE) mixture DE-71. Neurotoxicology 2009;30:326-329.

[33] Zou J, Wang YX, Dou FF, Lu HZ, Ma ZW, Lu PH, et al. Glutamine synthetase down-regulation reduces astrocyte protection against glutamate excitotoxicity to neurons. Neurochem Int 2010;56:577-584.

[34] Nagele RG, Wegiel J, Venkataraman V, Imaki H, Wang KC. Contribution of glial cells to the development of amyloid plaques in Alzheimer's disease. Neurobiol Aging 2004;25:663-674.

[35] Aliev G, Palacios HH, Lipsitt AE, Fischbach K, Lamb BT, Obrenovich ME, et al. Nitric oxide as an initiator of brain lesions during the development of Alzheimer disease. Neurotox Res 2009;16:293-305.

[36] Aliev G, Palacios HH, Walrafen B, Lipsitt AE, Obrenovich ME, Morales L. Brain mitochondria as a primary target in the development of treatment strategies for Alzheimer disease. Int J Biochem Cell Biol 2009;41:1989-2004.

[37] Garcia-Matas S, de Vera N, Aznar AO, Marimon JM, Adell A, Planas AM, et al. In vitro and in vivo activation of astrocytes by amyloid- beta is potentiated by pro-oxidant agents. J Alzheimers Dis 2010;20:229-245.

[38] Heales SJ, Lam AA, Duncan AJ, Land JM. Neurodegeneration or neuroprotection: the pivotal role of astrocytes. Neurochem Res 2004;29:513-519.

[39] Chiu IM, Chen A, Zheng Y, Kosaras B, Tsiftsoglou SA, Vartanian TK, et al. T lymphocytes potentiate endogenous neuroprotective inflammation in a mouse model of ALS. Proc Natl Acad Sci USA 2008;105:17913-17918.

[40] Chiu IM, Phatnani H, Kuligowski M, Tapia JC, Carrasco MA, Zhang M, et al. Activation of innate and humoral immunity in the peripheral nervous system of ALS transgenic mice. Proc Natl Acad Sci USA 2009;106:20960-20965.

[41] De Keyser J, Wilczak N, Leta R, Streetland C. Astrocytes in multiple sclerosis lack beta-2 adrenergic receptors. Neurology 1999;53:1628-1633.

[42] Zeinstra E, Wilczak N, De Keyser J. [3H]dihydroalprenolol binding to beta adrenergic receptors in multiple sclerosis brain. Neurosci Lett 2000;289:75-77.

[43] Barreto GE, Gonzalez J, Capani F, Morales L. Role of Astrocytes in Neurodegenerative Diseases. Neurodegenerative Diseases - Processes, Prevention, Protection and Monitoring 2011;257-272.

## 7. Appendices

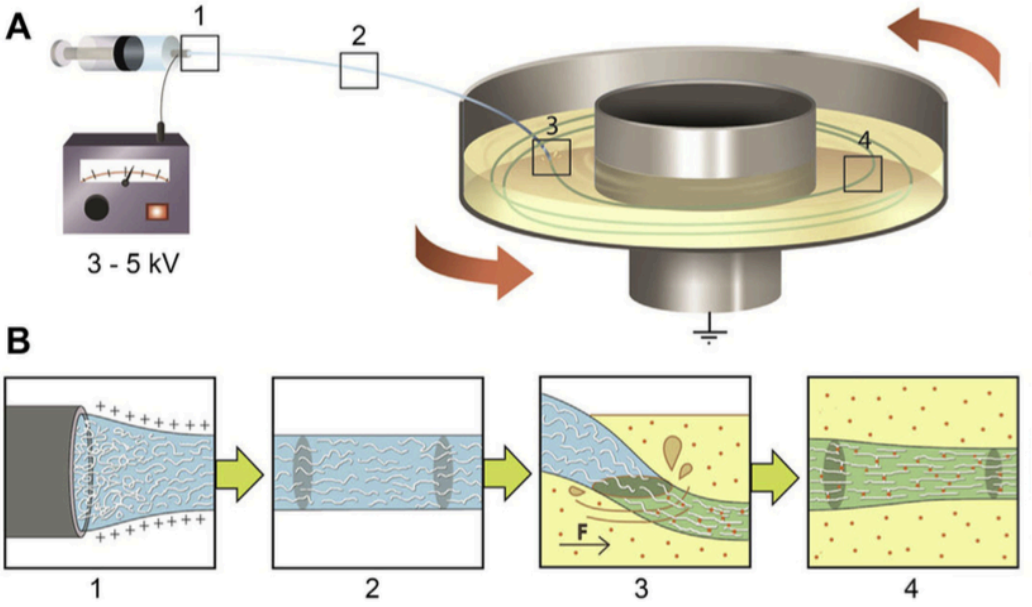


**Appendix 1.** Schematic of electrospinning set-up designed by Zhang *et al*. A polymer solution is extruded at a fixed rate from a syringe fitted with a blunted 27 G needle tip (**A**). A voltage between 3-5 kV is applied to the polymer solution, resulting in the formation of a Taylor cone as the applied electric field overcomes the solution viscosity (**B-1**). When the electrical field threshold has been surpassed, a finely charged polymer jet emerges from the tip of the Taylor cone and is stretched under the electrical force applied (**B-2**). The jet sprays as a continuous fiber onto a grounded, rotating collector filled with a cross-linking bath. The rotating wheel mechanically stretches the polymer jet (**B-3**). Fiber alignment is further induced as the polymer is rapidly cross-linked in the collection solution (**B-4**).[9]

## 8. Curriculum Vitae

Brook Jeang was born on December 9, 1992 in Monterey Park, CA and grew up in nearby Walnut, CA. In 2010, she graduated from Fairmont Preparatory Academy, where she was an Advanced Placement and International Baccalaureate student. She then attended Johns Hopkins University from 2010-2014, double majoring in Materials Science and Engineering and Applied Mathematics and Statistics. Brook completed her undergraduate senior design project in Dr. Hai-Quan Mao's lab, and continued working in the regenerative medicine subgroup of the Mao lab as she pursued her Master's in Materials Science and Engineering at JHU. She plans to apply her research and academic training in developing point-of-care diagnostic tools for developing countries following completion of her Master's in Science and Engineering degree.